

# Identifying and quantifying the impact of climatic and non-climatic drivers on river discharge in Europe

Julie Collignan<sup>1</sup>, Jan Polcher<sup>2</sup>, Sophie Bastin<sup>3</sup>, and Pere Quintana-Seguí<sup>4</sup>

<sup>1</sup>Laboratoire de Météorologie Dynamique/IPSL - Ecole Polytechnique/CNRS

<sup>2</sup>Laboratoire de Météorologie Dynamique/CNRS

<sup>3</sup>IPSL/LATMOS

<sup>4</sup>Observatori de l'Ebre (Universitat Ramon Llull - CSIC)

March 11, 2024

## Abstract

Our water resources have changed over the last century through a combination of water management evolutions and climate change. Understanding and decomposing these drivers of discharge changes is essential to preparing and planning adaptive strategies. We propose a methodology combining a physical-based model to reproduce the natural behavior of river catchments and a parsimonious model to serve as a framework of interpretation, comparing the physical-based model outputs to observations of discharge trends. We show that over Europe, especially in the South, the dominant explanations for discharge trends are non-climatic factors. Still, in some catchments of Northern Europe, climate change seems to be the dominating driver of change. We hypothesize that the dominating non-climatic factors are irrigation development, groundwater pumping and other human water usage, which need to be taken into account in physical-based models to understand the main drivers of discharge and project future changes.

1 **Identifying and quantifying the impact of climatic and**  
2 **non-climatic drivers on river discharge in Europe**

3 **Julie Collignan<sup>1</sup>, Jan Polcher<sup>1</sup>, Sophie Bastin<sup>2</sup>, Pere Quintana-Segui<sup>3</sup>**

4 <sup>1</sup>Laboratoire de Météorologie Dynamique/IPSL - Ecole Polytechnique/CNRS -, Paris, France

5 <sup>2</sup>Laboratoire Atmosphères, Observations Spatiales/IPSL - CNRS -, Paris, France

6 <sup>3</sup>Observatori de l'Ebre (Universitat Ramon Llull – CSIC), Roquetes, Spain

7 **Key Points:**

- 8 • Attribution of streamflow trends to climate drivers  
9 • Larger effect on streamflow of non-climatic drivers  
10 • Strong impact of human activities, especially over Spain

---

Corresponding author: Julie Collignan, [julie.collignan@lmd.ipsl.fr](mailto:julie.collignan@lmd.ipsl.fr)

## Abstract

Our water resources have changed over the last century through a combination of water management evolutions and climate change. Understanding and decomposing these drivers of discharge changes is essential to preparing and planning adaptive strategies. We propose a methodology combining a physical-based model to reproduce the natural behavior of river catchments and a parsimonious model to serve as a framework of interpretation, comparing the physical-based model outputs to observations of discharge trends. We show that over Europe, especially in the South, the dominant explanations for discharge trends are non-climatic factors. Still, in some catchments of Northern Europe, climate change seems to be the dominating driver of change. We hypothesize that the dominating non-climatic factors are irrigation development, groundwater pumping and other human water usage, which need to be taken into account in physical-based models to understand the main drivers of discharge and project future changes.

## Plain Language Summary

Water is an essential resource. Its access and management are key challenges in the context of climate change. Changes in precipitation distribution and intensity and other climate effects lead to a change in the water availability and in the discharge of rivers. On top of that, humans intervene to uptake water from rivers and change streamflow dynamics. To better assess management practices and prepare for future climate conditions, it is important to understand which part of discharge evolution is due to climate and which part is due to human intervention. In this article, we present an innovative methodology to do so. We show that over Europe, if discharge in the North is mostly impacted by the evolution of climate, in the rest, water management practices are the main cause of discharge changes. This is especially the case for the drying discharge trends in the South. Therefore, the evolution of management practices must be particularly of interest when constructing adaptation pathways to future climate conditions.

## 1 Introduction

Water is an essential resource for both ecosystems and human needs. Floods or water scarcity can lead to environmental catastrophes, conflicts and economic hardships. Understanding the evolution of water availability is a key challenge in the context of climate change and a highly managed continental water cycle. To study the evolution of water resources, one key variable is streamflow. Being at the surface, it is directly related to freshwater available to humans and ecosystems (Dai, 2016). In order to optimize its availability and reduce the impacts of floods and hydrological droughts, mankind has managed it over the last millennia. Because of its central role in our water resources, it has also been well observed over the last century.

From a geophysical perspective, streamflow provides a comprehensive overview of the water dynamics of catchments as it is the result of the catchment-integrated balance between water storage, precipitation and evapotranspiration (Milly et al., 2005; Rottler et al., 2020). These last two fluxes are dominated by climate processes and thus driven by atmospheric variability and trends (Christidis & Stott, 2022; García-Ruiz et al., 2011). On the other hand, it is through the management of water storage (reservoirs or groundwater pumping) and evaporation (land use and irrigation) that humans optimize the benefits they take from surface water and modify streamflows (Schneider et al., 2013; Riedel & Weber, 2020).

All of these processes have confounding effects on river discharge, which makes it difficult to detect and attribute trends in water resources (Rottler et al., 2020; Ficklin et al., 2018). With climate change, precipitation distribution, frequency and intensity are evolving, along with an increase in atmospheric water demand due to increased en-

60 ergy available at the surface and atmospheric water holding capacity and to changes in  
61 turbulences (Douveille et al., 2021; Christidis & Stott, 2022; García-Ruiz et al., 2011; Ribes  
62 et al., 2019; Dezsi et al., 2018). In turn, human activities and management, through ab-  
63 stractions (for irrigation, domestic uses...) and regulations (dams, reservoirs...), directly  
64 impact the partitioning of water between runoff and evapotranspiration along with flow  
65 seasonality, due to additional water uptakes and to controlled water releases (Rottler et  
66 al., 2020; García-Ruiz et al., 2011; Ficklin et al., 2018). Therefore, streamflow changes  
67 are driven by climate change and anthropogenic activities, both influencing catchment  
68 dynamics and equilibrium.

69 To project future streamflow changes and adapt water management strategies to  
70 climate change, it is essential first to understand the relative weight of these different  
71 drivers in streamflow dynamics. Being able to attribute past changes in river discharge  
72 to either climatic factors or human intervention on the land surface processes provides  
73 invaluable information to water managers in an evolving water cycle.

74 Physical-based land surface models (LSMs) and global hydrological models (GHMs)  
75 have been developed to understand streamflow dynamics, reproduce land surface pro-  
76 cesses and predict the evolution of the water cycle using different scenarios for the fu-  
77 ture (W. Zhao & Li, 2015; Nazemi & Wheatler, 2015). They have grown more complex  
78 over time and represent, at best, the current understanding of surface/atmosphere in-  
79 teractions, vegetation dynamics and hydrological processes under the control of climate  
80 (Tafasca et al., 2020; Quintana-Seguí et al., 2020; Stephens et al., 2023). These models  
81 are very useful to study patterns of change and trends and link them to specific processes  
82 (Douveille et al., 2021; Zanardo et al., 2012; Alkama et al., 2010; Do et al., 2020). How-  
83 ever, to this day, they fail to effectively include most anthropogenic water usage and man-  
84 agement, even if progress is being made in that direction (F. Wang et al., 2018; Nazemi  
85 & Wheatler, 2015).

86 In view of the complexity of land surface processes and the lack of data, another  
87 class of models has also been developed: parsimonious or calibrated models. Based on  
88 the perceived functioning of the surface hydrology (Beven & Chappell, 2021), relations  
89 and parameters are selected and then adjusted over a period to represent, at best, ac-  
90 tual streamflow characteristics. These models have demonstrated their value for oper-  
91 ational short-term predictions and to represent and detect current trends in discharge  
92 with a simplified interpretation tool (Jiang et al., 2015; Andréassian et al., 2016; Per-  
93 rin et al., 2003). However, they are limited in their ability to predict changes associated  
94 with specific drivers due to the difficulty of physical interpretation of the adjusted pa-  
95 rameters and the undetermined sensitivity of these parameters to the drivers (Zheng et  
96 al., 2018; Andréassian et al., 2016; Coron et al., 2014; Nicolle et al., 2021). Still they have  
97 been used to try and separate the effect of anthropogenic activities from climatic drivers,  
98 often comparing a reference "untouched" period or area to a post-change period or to  
99 a similar but highly anthropized area (Ficklin et al., 2018; W. Wang et al., 2020; Palmer  
100 et al., 2008; Ahn & Merwade, 2014; Zheng et al., 2018; Luo et al., 2020; J. Zhao et al.,  
101 2018). However, these methods all rely on the debatable assumption that the adjusted  
102 parameters are independent of climate variability (Coron et al., 2014; Andréassian et al.,  
103 2016; Reaver et al., 2022).

104 Using both classes of models, we propose a method to analyze observed annual river  
105 discharge and decompose observed trends into climate-driven changes and those caused  
106 by human intervention on the continental water cycle. The LSM is chosen as the climatic  
107 reference as it represents the behavior of catchments and land surface dynamics, respond-  
108 ing to changes in climate variables only. Due to the incomplete representation of the com-  
109 plex land surface processes and the lack of representation of human water management,  
110 the direct validation of the predicted river discharge to observation is difficult (Hagemann  
111 & Dümenil, 1997). The Budyko space and the one-parameter parsimonious model pro-  
112 posed by Fu's equation (Zhang et al., 2004) is used as a framework for interpreting both

113 the LSM’s simulated and the observed historical discharge. This parsimonious model in-  
 114 troduces a parameter allowing to isolate the partial trends in discharge ( $Q$ ) due to a change  
 115 in catchment evaporation efficiency from the partial trend due to changes in the two main  
 116 average climate variables precipitation ( $P$ ) and potential evapotranspiration ( $PET$ ) (Collignan,  
 117 Polcher, Bastin, & Quintana-Segui, 2023). Projecting the LSM output onto this frame-  
 118 work allows to derive the climate sensitivity of the adjusted parameter of the parsimo-  
 119 nious model. In turn, comparing these results to the interpretation of observed histor-  
 120 ical records by the Budyko model allows to isolate the trends due to changes in evap-  
 121 oration efficiency and land characteristics not represented by the LSM. This separates  
 122 the observed changes in streamflow into a component that can be attributed to climate  
 123 variations and another that can be linked to human activities.

## 124 2 Method

125 The Budyko framework is a relatively simple empirical framework which relies on  
 126 balancing the water and energy fluxes through only a few variables (precipitations  $P$  and  
 127 potential evapotranspiration  $PET$ ) to express the partitioning of water between evap-  
 128 otranspiration  $E$  and runoff. As opposed to other simple empirical models such as lin-  
 129 ear regression models, it accounts for physical boundaries: the water limit and the en-  
 130 ergy limit on the system. For the framework to work, it needs to be applied to a closed  
 131 system where the boundaries can be defined, such as a watersheds at an equilibrium state  
 132 (the variations of water storage within the catchment are supposed to be small). It is  
 133 simple enough to be applicable to a wide variety of observed catchments as only basic  
 134 variables are needed. In this study we used the parametric equation of Fu-Tixeront (Zhang  
 135 et al., 2004) (Zhang et al., 2008) (Zheng et al., 2018). It reduces for each catchment its  
 136 evaporation efficiency to a single specific parameter  $\omega$  (Equ. 1), fitted over hydrologi-  
 137 cal year averages, in a given period. For the same climatic conditions  $P$ ,  $PET$ , a catch-  
 138 ment with a higher  $\omega$  will evaporate more than another one with a smaller  $\omega$ .

139 In the original framework, this parameter is assumed to be constant since the wa-  
 140 tershed is considered to be in a stationary state and only driven by climate.

$$\frac{E}{P} = 1 + \frac{PET}{P} - \left( 1 + \left( \frac{PET}{P} \right)^\omega \right)^{\frac{1}{\omega}} \quad (1)$$

141  $E$  is the actual evaporation at the scale of the catchment. With the same assump-  
 142 tion of a closed system and no water storage change, the water continuity yields for dis-  
 143 charge  $Q = P - E$ .

144 Here, we consider only that the system is piece-wise stationary and that the pa-  
 145 rameter can be assumed to the constant over a short period (11 years) (Han et al., 2020).  
 146 This introduces a time-dependence in the parameter  $\omega$  by successive fits over an 11-year  
 147 time-moving window. We therefore capture the long-term effects of climate change and  
 148 anthropogenic activities, both influencing catchments responses.

149 As a result, both the annual mean of  $P$  and  $PET$ , regrouped in the variable  $C$  later  
 150 on, and for the evaporation efficiency  $\omega$  are time dependent. This allows to construct a  
 151 framework of interpretation, with a simple decomposition of discharge trends  $Q$ : a par-  
 152 tial trends due to long-term changes in average climate variable and a partial trend due  
 153 to changes in catchment responses. More details for this methodology are given in (Collignan,  
 154 Polcher, Bastin, & Quintana-Segui, 2023). In this framework, the anthropogenic water  
 155 management and water usage will only change the catchment responses and not the cli-  
 156 mate variables.

157 By applying the method to the observed catchments and the representation of these  
 158 catchments in a land surface model, the relative contribution of climate to trends in dis-  
 159 charge can be quantified. The two systems considered are :

- 160 • **A climate-driven system, referred as climatic system:** An LSM is used to  
 161 estimate the climate induced changes in the evaporation efficiency ( $\omega_c$ ). The LSM  
 162 stands as our climatic reference. It provides us with the following information:
  - 163 –  $\Delta Q_{climat}(C, \omega_c)$ : defined as the climate driven discharge trends.
  - 164 –  $\Delta Q_c(C, \overline{\omega_c})$ : partial trend due to fluctuations in annual averages of climate vari-  
 165 ables ( $C$ ), where  $\overline{\omega_c}$  is the average evaporation efficiency over the entire period.
  - 166 –  $\Delta Q_c(C_{rand}, \omega_c)$ : partial trend due to climatic impact on evaporation efficiency  
 167  $\omega_c$ , where  $C_{rand}$  is a random climate with no trends.
- 168 • **The observation-based system, referred as actual system:** the framework  
 169 is used to decompose the observed discharge changes. We successively fit the frame-  
 170 work to discharge observations, getting another time series of the evaporation ef-  
 171 ficiency parameter  $\omega_a$ . This provides the following information:
  - 172 –  $\Delta Q_{actual}(C, \omega_a)$ : overall trend in  $Q$  in the actual system.
  - 173 –  $\Delta Q_a(C, \overline{\omega_a})$ : partial trend due to changes in  $C$ .
  - 174 –  $\Delta Q_a(C_{rand}, \omega_a)$ : By randomizing the climate, the partial trend due to the evo-  
 175 lution of evaporation efficiency  $\omega_a$  can be estimated. In that case, all changes  
 176 in the watershed characteristics (anthropogenic as well as its climate in-  
 177 duced) are considered.

178 We illustrate the differences in both systems over a given catchment, with a fig-  
 179 ure of  $Q_{climat}$ ,  $Q_{actual}$ ,  $\omega_c$  and  $\omega_a$ , for the station of Castejon, upstream of the Ebro river  
 180 in Spain (in supplementary materials, Fig. S3).

181 We consider that the LSM accurately reproduces dynamic changes in an idealized  
 182 natural catchment driven by observed climatic conditions, even if it might have biases  
 183 in the absolute values of discharge. Therefore we only compare trends between both sys-  
 184 tems. All trends are computed using the Mann-Kendall non-parametric test, associated  
 185 with the Thiel-Sen slope estimator (Xiong et al., 2020), with a 0.05 p-value threshold  
 186 for significance.

## 187 3 Data

### 188 3.1 The Land Surface Model ORCHIDEE

189 The LSM used in this study is the Organizing Carbon and Hydrology In Dynamic  
 190 Ecosystems (ORCHIDEE) (Krinner et al., 2005) from the Institut Pierre Simon Laplace  
 191 (IPSL). The current version of the model simulates the global carbon cycle and quan-  
 192 tifies terrestrial water and energy balance through biophysical and natural biogeochem-  
 193 ical processes. It can include some anthropogenic interference such as land cover changes,  
 194 forest and grassland management or irrigation (Guimberteau et al., 2012). Here the model  
 195 is used without these options, as only the climatic dependences of hydrology are sought.  
 196 Used in off-line conditions, the atmospheric conditions are forced by a given data-set.

### 197 3.2 Forcing datasets

198 Three different climatic datasets are used to drive the LSM. These datasets are used  
 199 as input to the off-line LSM and provide the variables needed in Fu's equation 1. The  
 200 main one is the forcing dataset GSWP3 (Hyungjun, 2017), covering the 1901-2012 pe-  
 201 riod at a 3-hourly resolution with a geographic resolution of  $0.5^\circ \times 0.5^\circ$ . It is a dynam-  
 202 ical downscaling of 20th Century Reanalysis using a Global Spectral Model. It is bias-  
 203 corrected using Global Precipitation Climatology Center (GPCC) (Rudolf et al., 2005)  
 204 and Climate Research Unit (CRU) observational data (Harris et al., 2020). The results  
 205 presented later on are obtained with this forcing dataset.

We also use two other forcings, WFDEI-GPCC (Weedon et al., 2014) and E2OFD (Beck et al., 2017), both covering the 1979 to 2014 period. Testing the methodology with different independent climate datasets allows to verify the robustness of our results comparing the two systems and their sensitivity to the choice of climate forcing used (see supplementary materials).

### 3.3 Watersheds and discharge observation datasets

The river discharge observations collected by the Global Runoff Data Center (GRDC) from gauging stations all over Europe (GRDC, 2020) are the base of the current study. They were completed over Spain with data obtained from the Geoportail of Spain Ministerio (Ministerio para la Transición Ecológica y el Reto Demográfico, 2020) and over France with data from the database HYDRO (Ministere de l'ecologie, du developpement durable et de l'energie, 2021). In the final analysis, only 814 stations were kept with at least 50 years of observations and for which we were able to satisfyingly reproduce the upstream catchment in the hydrological routing of the LSM (Polcher et al., 2022; Nguyen-Quang et al., 2018), based on the dataset HydroSHEDS (Hydrological Data and Maps Based on Shuttle Elevation Derivatives at Multiple Scales) (Lehner et al., 2008).

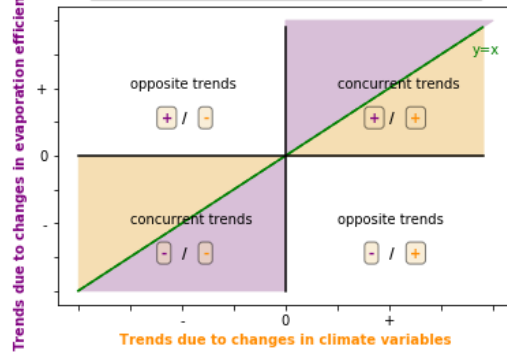
## 4 Results

### 4.1 Decomposing the trends in river discharge over the past century

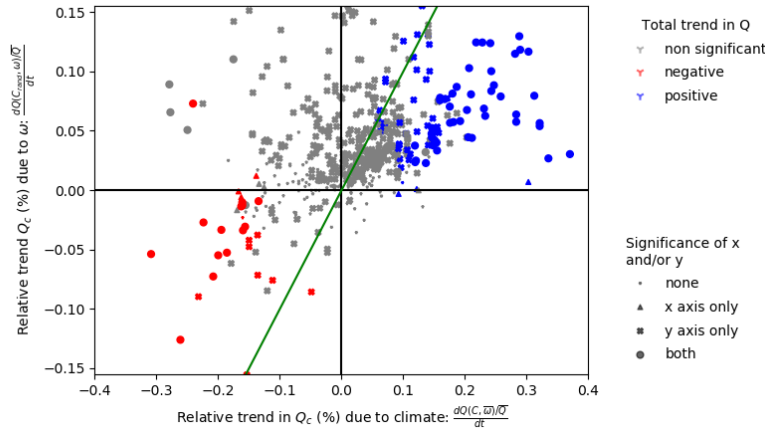
The framework defined by the parsimonious model chosen allows to separate trends in river discharge ( $Q$ ) into the part explained by the evolution of climate  $C$  (x-axis) and a partial trend due to changes in the catchment affecting evaporation efficiency ( $\omega$ ) (y-axis). Figure 1a allows to illustrate the relative importance of both components of the trends as estimated with the methodology presented above, using a 100-year-long simulation with an LSM and the observed discharge at 569 gauging stations.

Positioning the results for one catchment in Fig. 1a allows to illustrate the magnitudes of the partial trends due to each component and whether they are concurrent or opposite and if they tend to increase or decrease discharge. Two different systems are projected on this framework for comparison (see Method): the climatic system ( $Q_{climat}$ ) based on the LSM outputs and the actual system ( $Q_{actual}$ ) based on observed records.

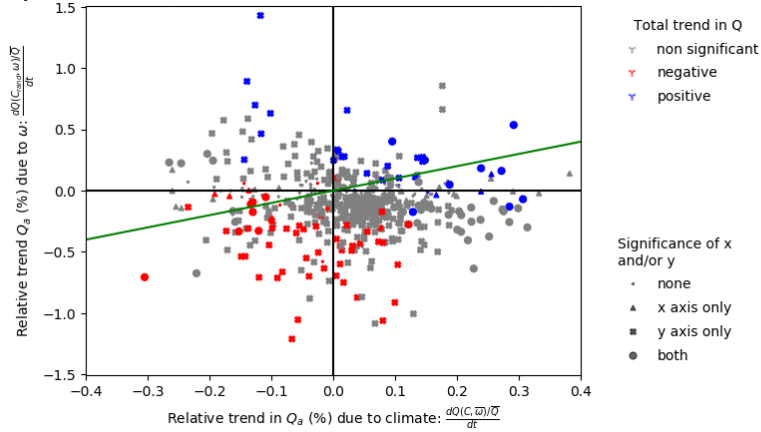
Our results show that in the case of the climatic system (Fig. 1b), the changes in annual mean climate variables have about a four times larger impact than the changes in evaporation efficiency on relative annual mean discharge trends. Overall, almost all catchments where  $Q_{climat}$  has significantly changed (catchments with significant trends correspond to colored points) have concurrent trends in both components. A high covariance between these two components allows to better detect the trends. More generally, there is a dominance of the trends in annual mean in climate variables  $P$ ,  $PET$ , amplified by the response of evaporation efficiency of the catchment induced by climate change. These cases correspond to catchments where an increase in  $P$  and/or a decrease in  $PET$  tends to increase annual mean discharge or inversely for a decrease. For instance, if an increase in  $P$  is inhomogeneous, with an even stronger increase in winter precipitation, the partitioning towards runoff is usually higher, which translates into a decreased evaporation efficiency and thus an even stronger increase of  $Q_{climat}$  (top right quadrant, Fig. 1b). Therefore in this example, the increase in the annual mean  $Q_{climat}$  is not only due to an increase in annual mean  $P$  but is amplified by the more contrasted seasonality and its impact on evaporation efficiency. More generally, there are fewer catchments where the changes in the evaporation efficiency tend to decrease discharge in the climatic system, except when they concur with a high decrease in relative discharge due to a decrease in  $P$  and/or an increase in  $PET$ . This is coherent with the increasing intensity and contrasted seasonality of precipitation events observed over Europe (Christidis &



(a) Interpretation scheme: comparing significant trends due to climate variables or due to  $\omega$ . The graphs have four quadrants: the top right and the bottom left ones correspond to area of the graph where the climatic trend and the area due to  $\omega$  are complementary/ going into the same direction. The top left one contains the basins for which the trends due to  $\omega$  are positive and the trends due to climate variables are negative and the bottom right quadrant the opposite.



(b) Climatic system  $Q_{climat}$ : relative trends (%/yr over the century) due to changes in  $\omega_c$  versus relative trends due to changes in climate variables  $C$



(c) Actual system  $Q_{actual}$ : relative trends (%/yr over the century) due to changes in  $\omega_a$  versus relative trends due to changes in climate variables  $C$

**Figure 1.** Comparing the relative trends ( $\frac{dQ}{dt}/\bar{Q}$ ) due to a change in climate variables or due to a change in evaporation efficiency  $\omega$  in the evolution of discharge, for both system  $Q_{climat}$  and  $Q_{actual}$ . One point corresponds to a basin with at least 50 years of river discharge observations over Europe. The scale of trends due to  $\omega_a$  in the actual system is ten times larger than the one for trends due to  $\omega_c$  in the climatic system. The green line is the line  $y = x$ . The color scale represents the significance of the trend in  $Q$  when all factors are considered. The markers indicate whether the partial trends are significant due to changes in  $C$  (x-axis), in  $\omega$  (y-axis), or both.

255 Stott, 2022; Riedel & Weber, 2020; Zveryaev, 2004; Ribes et al., 2019; Douville et al.,  
 256 2021), which would logically tend to decrease evaporation efficiency by increasing local  
 257 runoff, and therefore lead to a positive partial trend in discharge.

258 In the case of the observed system (Fig. 1c), the relationship between the two partial  
 259 trends looks very different. The one linked to changes in evaporation efficiency is larger  
 260 than the partial trends linked to the annual mean in  $P$  and  $PET$  by a factor of 3. More  
 261 generally, the total trends in  $Q_{actual}$  (catchments with significant trends correspond to  
 262 colored points) follow the partial trends due to changes in the catchments' evaporation  
 263 efficiency. Therefore, in the actual system, the trends in discharge are mainly due to changes  
 264 in catchment behavior due to non-climatic factors. Contrary to when only climate change  
 265 is considered for natural catchments, land use changes and human water management  
 266 tend to increase the evaporation efficiency of catchments and, therefore, decrease  $Q_{actual}$ .  
 267 This is coherent with activities such as irrigation, or agriculture in general, which aim  
 268 at optimizing the evapotranspiration over catchments.

## 269 4.2 Geographical distribution of discharge trend characteristics

270 The spatial distribution of the significant relative trends (Fig. 2) is spatially coher-  
 271 ent, which also attests to the method's robustness. When some specific catchments  
 272 are referred to, the geographic location of these catchments is illustrated in supplement-  
 273 ary material (Fig. S2).

274 In the climatic system (Fig. 2a), basins in eastern Europe and Spain are getting  
 275 dryer with trends in discharge between  $-0.2\%/yr$  and  $-0.5\%/yr$  over the past century. In  
 276 central and northern Europe, the climatic discharge is increasing with trends of  $+0.2\%/yr$   
 277 to  $0.5\%/yr$  over the past century. Similarly to the previous results, we observe that in  
 278 this system, the trends in discharge  $Q_{climat}$  (Fig. 2a) are mostly driven by changes in  
 279 average climate variables  $C$  (Fig. 2c) and not to changes in evaporation efficiency  $\omega_c$  (Fig.  
 280 2e). These partial trends due to changes in the evaporation efficiency  $\omega_c$  (Fig. 2e) are  
 281 small (between  $-0.2\%/yr$  to  $+0.2\%/yr$ ) and are mostly positive. Their effect is negligi-  
 282 ble when looking at the total trends in discharge (Fig. 2a). It can however amplify the  
 283 partial trend due to changes in the annual average of climate variables  $C$ . It corresponds  
 284 to the top-right and bottom-left quadrants in Fig. 1b. This effect is illustrated in the  
 285 Duero basin in north-western Spain, where both partial trends concur to a decrease in  
 286  $Q_{climat}$ . They can also cancel each other out, for instance, in the Tiber River in Italy,  
 287 where the decrease in  $Q_{climat}$  due to changes in  $C$  is not significant in the overall changes  
 288 in  $Q_{climat}$ .

289 Again, for the actual system, our results show that the discharge trends (Fig. 2b)  
 290 are mostly explained by changes in the evaporation efficiencies (Fig. 2f). Here the changes  
 291 in the evaporation efficiency  $\omega_a$  encompass all changes in the catchment's evaporative  
 292 behaviors, those induced by climate and those by changing water usage. Similarly to re-  
 293 sults from other studies (Vicente-Serrano et al., 2019) over Western Europe, we find the  
 294 highest negative trends are over Southern Spain and are mostly driven by non-climatic  
 295 factors. To facilitate the comparison, scales of the Fig. 2 are fixed thus for Fig. 2d and  
 296 Fig. 2f they saturate, not showing that the trends are a lot higher in Spain, with up to  
 297  $-4.4\%/yr$  change over the past century in  $Q_{actual}$ . Over the rest of Europe, trends are  
 298 lower and less significant, with positive trends generally in northern Europe, Great Britain  
 299 and Sweden and negative trends over central Europe. The south of Spain corresponds  
 300 to an area where both climate changes and changes related to human activities led to  
 301 a significant decrease in river discharge over the past century. There, mainly, the changes  
 302 in evaporation efficiency result in decreasing trends in  $Q_{actual}$  (Fig. 2f). This is coher-  
 303 ent with increasing irrigation water uptakes. However, the Guadiana River stands out  
 304 in our results. It seems that over that specific catchment, the overall effect of human wa-  
 305 ter management and land use changes tend to increase  $Q_{actual}$ , contrary to the rest of

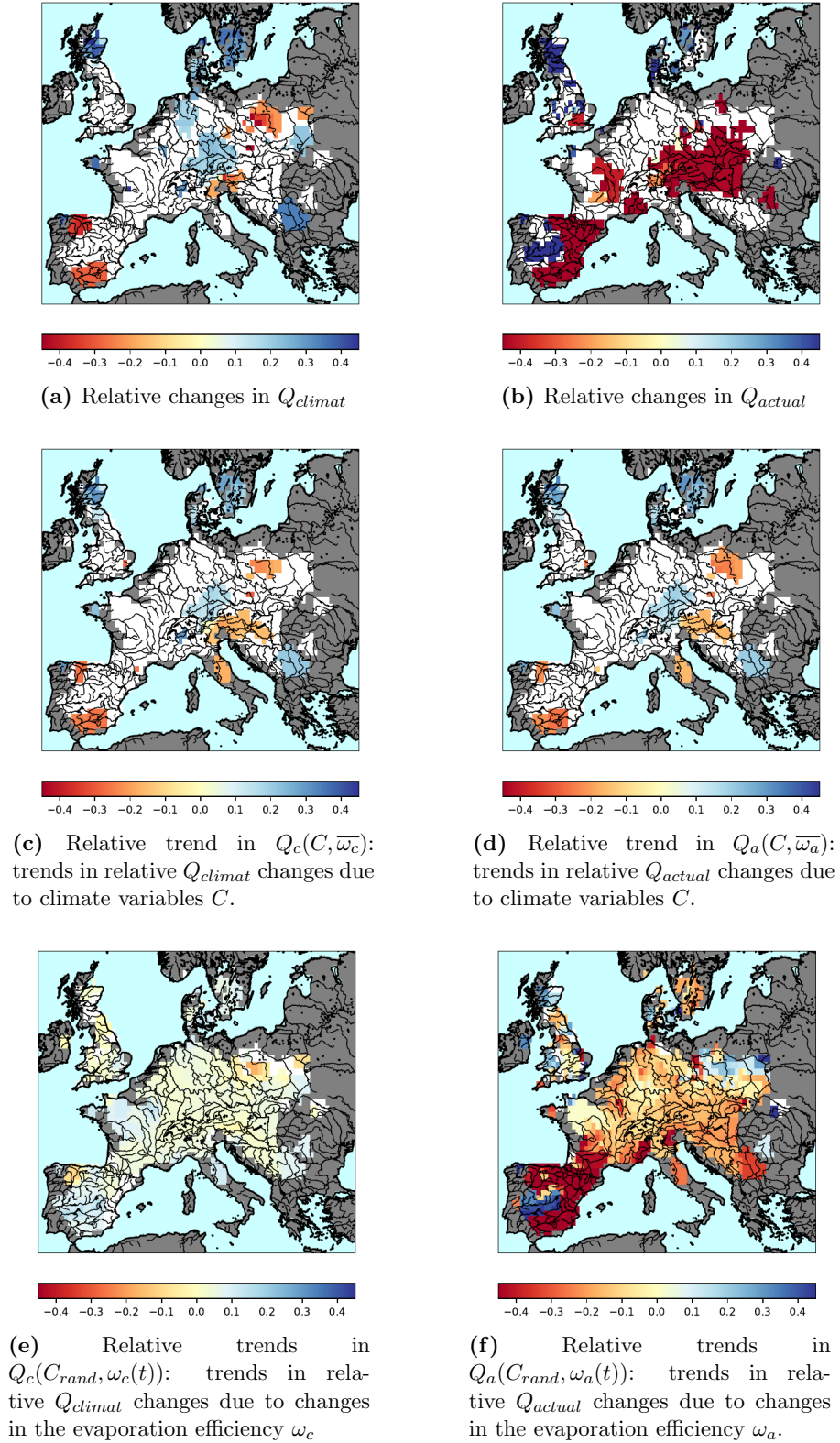


**Figure 2.** Significant trends in the relative river discharge  $Q/\bar{Q}$  over the time period 1901-2012 (%/yr over the century). The scales have been forced to be the same for all maps for comparison purposes but the extrema can go higher or lower.

Spain. As discussed later, this could be linked to unsustainable groundwater pumping (Holtz & Pahl-Wostl, 2012), which invalidates the hypothesis of no water storage change and, therefore, results in a lower apparent evaporation efficiency and an artificially underestimated evapotranspiration, increasing the resulting discharge. More generally, there are several basins over Europe where the trends induced by changes in the evaporation efficiency lose their significance when the climate variability is considered in the reconstructed discharge. See, for instance, western France, northern Germany, Serbia.

Interestingly, when we draw similar maps for sub-periods of 10 years, the impact of evaporation efficiency changes on discharge is not dominant anymore. At the decadal scale, the climatic variability is high. This climatic noise covers the effect of changes in the catchment's evaporation efficiency in discharge trends. At the scale of the century, the signal-to-noise ratio is higher, bringing to light the long-term role of changes in the catchment's evaporation efficiency and catchment's behavior on discharge.

## 5 Discussion

Our method uses a parsimonious hydrological model to decompose the observed river discharge trends into climate-driven processes, as estimated with a state-of-the-art LSM, and non-climatic changes that can be attributed to human activities. It can be generalized to the use of any couple of calibrated parsimonious model and physical-based model and be an effective operational tool to estimate and illustrate the effect of non-climatic drivers and land surface changes not well accounted for in current models and which may have a strong direct impact on water resources.

We show that the dominant explanation for river discharge trends is non-climatic factors, especially in Southern Europe. In some catchments of Northern Europe, climate change seems to be the dominating driver of change. Still, in accordance with previous studies (Gudmundsson et al., 2017), our results highlight the fact that not accounting for non-climatic trends leads to high under-estimation of discharge changes in the physical-based model used and therefore to high uncertainties in projections of future water resource trends, especially when looking at long-term trends.

With this methodology, we can only estimate the magnitude of non-climatic trends but not attribute them to specific processes. In some areas where a dominant process can be hypothesized, such as irrigation, correlation with indicators can allow to verify the plausibility of the assumed cause. For instance, over Spain, especially over the Ebro basin, the strong increase in evaporation efficiency and reduced discharge is correlated to the development of dams with a coefficient above 0.7 when correlating  $\omega_a$  to reservoirs levels for 6 sub-basins in this catchment. Dams water storage is an indicator for human management of water resources impacting the evaporation efficiency of watersheds. More generally, we see that the changes in the evaporation efficiency intensified over the second part of the century, where areas equipped for irrigation have been developed (Angelakis et al., 2020; Siebert et al., 2015). However, the available data are insufficient to attest to a correlation with that latter factor or with the effective amount of water used for irrigation. Groundwater pumping and glacier melt can explain positive trends in discharge due to additional sources of water not accounted for in the climatic system, which lead to artificially low evaporation efficiencies in our framework. For the Guadiana River in Spain, the unsustainable groundwater pumping (Holtz & Pahl-Wostl, 2012; Llamas et al., 2015; Esteban & Albiac, 2012) can explain the positive trend. In a similar way, for the Po river in Italy, which is highly irrigated (Siebert et al., 2015), we would expect a strong decrease in discharge as in most of Spain, but glacier melt brings additional water to the system (Schaner et al., 2012; Vincent et al., 2017; Huss & Hock, 2018), explaining a reduced detected negative trend over the end of the century. Other phenomena, such as soil sealing and river management, would be expected to have similar effects due to a decrease in evapotranspiration or to an artificial enhancement of runoff.

357 Changes in land use as represented in ORCHIDEE (Lawrence et al., 2016) are shown  
 358 to have little effect on discharge over the studied period and area but could have a more  
 359 significant effect at finer scale over small catchments.

360 Quantifying the contribution of climatic and non-climatic factors to changes in river  
 361 discharge is an important first step. But it should be followed by an attribution. The  
 362 use of the LSM in its current state allows to attribute the changes due to climate. How-  
 363 ever, the non-climatic factors remain challenging to attribute to specific processes, es-  
 364 pecially since most factors have concurring and competing effects. Detection and attri-  
 365 bution methods have been developed in climate studies to assess anthropogenic climate  
 366 change. They have allowed to determine the role of different factors by reproducing them  
 367 first in GCMs (Hegerl & Zwiers, 2011; Douville et al., 2021). Similarly, we would need  
 368 to simulate water usage such as irrigation, dam management, groundwater pumping and  
 369 other missing phenomena such as glacier melting in the LSMs so that their impact on  
 370 the evaporation efficiency can be identified and their contribution to the non-climatic  
 371 trend quantified.

372 Understanding and quantifying the contribution of various processes contributing  
 373 to observed discharge changes over the past century is an essential step in developing adap-  
 374 tation strategies to face climate change. In the future, changes in climatic variables are  
 375 expected to increase even further, with increase in intense precipitation events (Ribes  
 376 et al., 2019; Douville et al., 2021), an increase in evaporative demand and especially a  
 377 decrease in average precipitation leading to water scarcity over southern Mediterranean  
 378 Europe (Gudmundsson et al., 2017; Alkama et al., 2013). Concurrently, in Europe, hu-  
 379 man water management is expected to evolve to adapt to climate change and other con-  
 380 straints, such as changes in water and energy demand and regulations (Arheimer et al.,  
 381 2017). For instance, the extent of irrigated land in Europe peaked at the end of the 20th  
 382 century and the future irrigation evolution is expected to follow new goals and mostly  
 383 rely on improved efficiency (Adeyeri et al., 2020). Therefore, the balance between the  
 384 different terms influencing catchment evaporation efficiency and discharge may change.  
 385 If non-climatic factors dominated over the past century to explain discharge trends, it  
 386 may not be the same in the future. Attribution needs to be tested over the documented  
 387 past to improve the representation of non-climatic processes and allow the effective pro-  
 388 jection of future evolutions and eventual changes in this balance.

## 389 Open Research Section

390 The outputs of the LSM ORCHIDEE for each catchment used in this study with  
 391 the forcing GSWP3 are gathered in a file freely available on Zenodo.org (Collignan, Polcher,  
 392 Bastin, & Quintana-Seguí, 2023). This file also contains the description of the stations  
 393 used in the study: their location, the size of the upstream area used to position the sta-  
 394 tion on the grid and annual averages of streamflow observations.

## 395 Acknowledgments

396 We would like to acknowledge the support of the Agence Nationale de la Recherche un-  
 397 der contract HLIaise (ANR-19-CE01-0017-02). The lead author would like to thank  
 398 Institut Polytechnique de Paris for the Gaspard Monge fellowship, which funded her PhD  
 399 thesis.

## 400 References

- 401 Adeyeri, O. E., Laux, P., Lawin, A. E., & Arnault, J. (2020, March). Assessing  
 402 the impact of human activities and rainfall variability on the river discharge  
 403 of Komadugu-Yobe Basin, Lake Chad Area. *Environmental Earth Sciences*,  
 404 79(6), 143. doi: 10.1007/s12665-020-8875-y

- 405 Ahn, K.-H., & Merwade, V. (2014, July). Quantifying the relative impact of climate  
406 and human activities on streamflow. *Journal of Hydrology*, *515*, 257–266. doi:  
407 10.1016/j.jhydrol.2014.04.062
- 408 Alkama, R., Kageyama, M., & Ramstein, G. (2010). Relative contributions of  
409 climate change, stomatal closure, and leaf area index changes to 20th and  
410 21st century runoff change: A modelling approach using the Organizing  
411 Carbon and Hydrology in Dynamic Ecosystems (ORCHIDEE) land surface  
412 model. *Journal of Geophysical Research: Atmospheres*, *115*(D17). doi:  
413 10.1029/2009JD013408
- 414 Alkama, R., Marchand, L., Ribes, A., & Decharme, B. (2013, July). Detec-  
415 tion of global runoff changes: Results from observations and CMIP5 ex-  
416 periments. *Hydrology and Earth System Sciences*, *17*(7), 2967–2979. doi:  
417 10.5194/hess-17-2967-2013
- 418 Andréassian, V., Coron, L., Lerat, J., & Le Moine, N. (2016, November). Climate  
419 elasticity of streamflow revisited – an elasticity index based on long-term hy-  
420 drometeorological records. *Hydrology and Earth System Sciences*, *20*(11),  
421 4503–4524. doi: 10.5194/hess-20-4503-2016
- 422 Angelakis, A. N., Zaccaria, D., Krasilnikoff, J., Salgot, M., Bazza, M., Roccaro, P.,  
423 ... Fereres, E. (2020, May). Irrigation of World Agricultural Lands: Evolution  
424 through the Millennia. *Water*, *12*(5), 1285. doi: 10.3390/w12051285
- 425 Arheimer, B., Donnelly, C., & Lindström, G. (2017, July). Regulation of snow-fed  
426 rivers affects flow regimes more than climate change. *Nature Communications*,  
427 *8*(1), 62. doi: 10.1038/s41467-017-00092-8
- 428 Beck, H. E., van Dijk, A. I. J. M., Levizzani, V., Schellekens, J., Miralles, D. G.,  
429 Martens, B., & de Roo, A. (2017, January). MSWEP: 3-hourly 0.25°&deg;  
430 global gridded precipitation (1979–2015) by merging gauge, satellite,  
431 and reanalysis data. *Hydrology and Earth System Sciences*, *21*(1), 589–615.  
432 doi: 10.5194/hess-21-589-2017
- 433 Beven, K. J., & Chappell, N. A. (2021). Perceptual perplexity and parameter parsimony.  
434 *WIREs Water*, *8*(4), e1530. doi: 10.1002/wat2.1530
- 435 Christidis, N., & Stott, P. A. (2022, August). Human Influence on Seasonal Precipitation  
436 in Europe. *Journal of Climate*, *35*(15), 5215–5231. doi: 10.1175/JCLI-D  
437 -21-0637.1
- 438 Collignan, J., Polcher, J., Bastin, S., & Quintana-Segui, P. (2023). Budyko Frame-  
439 work Based Analysis of the Effect of Climate Change on Watershed Evapora-  
440 tion Efficiency and Its Impact on Discharge Over Europe. *Water Resources*  
441 *Research*, *59*(10), e2023WR034509. doi: 10.1029/2023WR034509
- 442 Collignan, J., Polcher, J., Bastin, S., & Quintana-Seguí, P. (2023, August). *Out-*  
443 *put of the Land Surface Model ORCHIDEE over river catchments in Europe,*  
444 *run with GSWP3 and synthetic forcings where the precipitation is modified.*  
445 Zenodo. doi: 10.5281/zenodo.8211025
- 446 Coron, L., Andréassian, V., Perrin, C., Bourqui, M., & Hendrickx, F. (2014, Febru-  
447 ary). On the lack of robustness of hydrologic models regarding water balance  
448 simulation: A diagnostic approach applied to three models of increasing com-  
449 plexity on 20 mountainous catchments. *Hydrology and Earth System Sciences*,  
450 *18*(2), 727–746. doi: 10.5194/hess-18-727-2014
- 451 Dai, A. (2016). Historical and Future Changes in Streamflow and Continental  
452 Runoff. In *Terrestrial Water Cycle and Climate Change* (pp. 17–37). American  
453 Geophysical Union (AGU). doi: 10.1002/9781118971772.ch2
- 454 Dezi, Ş., Mindrescu, M., Petrea, D., Rai, P. K., Hamann, A., & Nistor, M.-M.  
455 (2018). High-resolution projections of evapotranspiration and water availabil-  
456 ity for Europe under climate change. *International Journal of Climatology*,  
457 *38*(10), 3832–3841. doi: 10.1002/joc.5537
- 458 Do, H. X., Zhao, F., Westra, S., Leonard, M., Gudmundsson, L., Boulange, J. E. S.,  
459 ... Wada, Y. (2020, April). Historical and future changes in global flood

- 460 magnitude – evidence from a model–observation investigation. *Hydrology and*  
 461 *Earth System Sciences*, 24(3), 1543–1564. doi: 10.5194/hess-24-1543-2020
- 462 Douville, H., Raghavan, K., Renwick, J., Allan, R., Arias, P., Barlow, M., . . . Zolina,  
 463 O. (2021). Water Cycle Changes. In *Climate Change 2021: The Physical*  
 464 *Science Basis. Contribution of Working Group I to the Sixth Assessment Re-*  
 465 *port of the Intergovernmental Panel on Climate Change.*, 1055–1210. doi:  
 466 10.1017/9781009157896.010
- 467 Esteban, E., & Albiac, J. (2012, August). The problem of sustainable groundwa-  
 468 ter management: The case of La Mancha aquifers, Spain. *Hydrogeology Jour-*  
 469 *nal*, 20(5), 851–863. doi: 10.1007/s10040-012-0853-3
- 470 Ficklin, D. L., Abatzoglou, J. T., Robeson, S. M., Null, S. E., & Knouft, J. H. (2018,  
 471 August). Natural and managed watersheds show similar responses to recent  
 472 climate change. *Proceedings of the National Academy of Sciences*, 115(34),  
 473 8553–8557. doi: 10.1073/pnas.1801026115
- 474 García-Ruiz, J. M., López-Moreno, J. I., Vicente-Serrano, S. M., Lasanta-Martínez,  
 475 T., & Beguería, S. (2011, April). Mediterranean water resources in a  
 476 global change scenario. *Earth-Science Reviews*, 105(3), 121–139. doi:  
 477 10.1016/j.earscirev.2011.01.006
- 478 Gudmundsson, L., Seneviratne, S. I., & Zhang, X. (2017, November). Anthropogenic  
 479 climate change detected in European renewable freshwater resources. *Nature*  
 480 *Climate Change*, 7(11), 813–816. doi: 10.1038/nclimate3416
- 481 Guimberteau, M., Laval, K., Perrier, A., & Polcher, J. (2012, September). Global  
 482 effect of irrigation and its impact on the onset of the Indian summer monsoon.  
 483 *Climate Dynamics*, 39(6), 1329–1348. doi: 10.1007/s00382-011-1252-5
- 484 Hagemann, S., & Dümenil, L. (1997, December). A parametrization of the lateral  
 485 waterflow for the global scale. *Climate Dynamics*, 14(1), 17–31. doi: 10.1007/  
 486 s003820050205
- 487 Han, J., Yang, Y., Roderick, M. L., McVicar, T. R., Yang, D., Zhang, S., & Beck,  
 488 H. E. (2020). Assessing the Steady-State Assumption in Water Balance  
 489 Calculation Across Global Catchments. *Water Resources Research*, 56(7),  
 490 e2020WR027392. doi: 10.1029/2020WR027392
- 491 Harris, I., Osborn, T. J., Jones, P., & Lister, D. (2020, April). Version 4 of the  
 492 CRU TS monthly high-resolution gridded multivariate climate dataset. *Scien-*  
 493 *tific Data*, 7(1), 109. doi: 10.1038/s41597-020-0453-3
- 494 Hegerl, G., & Zwiers, F. (2011). Use of models in detection and attribution of cli-  
 495 mate change. *WIREs Climate Change*, 2(4), 570–591. doi: 10.1002/wcc.121
- 496 Holtz, G., & Pahl-Wostl, C. (2012, March). An agent-based model of groundwa-  
 497 ter over-exploitation in the Upper Guadiana, Spain. *Regional Environmental*  
 498 *Change*, 12(1), 95–121. doi: 10.1007/s10113-011-0238-5
- 499 Huss, M., & Hock, R. (2018, February). Global-scale hydrological response to future  
 500 glacier mass loss. *Nature Climate Change*, 8(2), 135–140. doi: 10.1038/s41558  
 501 -017-0049-x
- 502 Hyungjun, K. (2017). Global Soil Wetness Project Phase 3 Atmospheric Boundary  
 503 Conditions (Experiment 1). *Data Integration and Analysis System (DIAS)*, 5.  
 504 doi: doi:10.20783/DIAS.501
- 505 Jiang, C., Xiong, L., Wang, D., Liu, P., Guo, S., & Xu, C.-Y. (2015, March). Sepa-  
 506 rating the impacts of climate change and human activities on runoff using the  
 507 Budyko-type equations with time-varying parameters. *Journal of Hydrology*,  
 508 522, 326–338. doi: 10.1016/j.jhydrol.2014.12.060
- 509 Krinner, G., Viovy, N., de Noblet-Ducoudré, N., Ogée, J., Polcher, J., Friedlingstein,  
 510 P., . . . Prentice, I. C. (2005). A dynamic global vegetation model for studies  
 511 of the coupled atmosphere-biosphere system. *Global Biogeochemical Cycles*,  
 512 19(1). doi: 10.1029/2003GB002199
- 513 Lawrence, D. M., Hurtt, G. C., Arneth, A., Brovkin, V., Calvin, K. V., Jones,  
 514 A. D., . . . Shevliakova, E. (2016, September). The Land Use Model Inter-

- 515 comparison Project (LUMIP) contribution to CMIP6: rationale and exper-  
 516 imental design. *Geoscientific Model Development*, 9(9), 2973–2998. doi:  
 517 10.5194/gmd-9-2973-2016
- 518 Lehner, B., Verdin, K., & Jarvis, A. (2008). New Global Hydrography Derived From  
 519 Spaceborne Elevation Data. *Eos, Transactions American Geophysical Union*,  
 520 89(10), 93–94. doi: 10.1029/2008EO100001
- 521 Llamas, M. R., Custodio, E., de la Hera, A., & Fornés, J. M. (2015, March).  
 522 Groundwater in Spain: Increasing role, evolution, present and future. *Envi-  
 523 ronmental Earth Sciences*, 73(6), 2567–2578. doi: 10.1007/s12665-014-4004-0
- 524 Luo, Y., Yang, Y., Yang, D., & Zhang, S. (2020, November). Quantifying the impact  
 525 of vegetation changes on global terrestrial runoff using the Budyko framework.  
 526 *Journal of Hydrology*, 590, 125389. doi: 10.1016/j.jhydrol.2020.125389
- 527 Milly, P. C. D., Dunne, K. A., & Vecchia, A. V. (2005, November). Global pat-  
 528 tern of trends in streamflow and water availability in a changing climate. *Na-  
 529 ture*, 438(7066), 347–350. doi: 10.1038/nature04312
- 530 Ministère de l’écologie, du développement durable et de l’énergie. (2021). *HYDRO*  
 531 [Dataset]. <https://www.hydro.eaufrance.fr/rechercher/entites-hydrometriques>.
- 532 Ministerio para la Transición Ecológica y el Reto Demográfico. (2020). *GeoPortal*.  
 533 <https://www.miteco.gob.es/es/cartografia-y-sig/ide/geoportal.html>.
- 534 Nazemi, A., & Wheeler, H. S. (2015, January). On inclusion of water resource  
 535 management in Earth system models &ndash; Part 1: Problem definition and  
 536 representation of water demand. *Hydrology and Earth System Sciences*, 19(1),  
 537 33–61. doi: 10.5194/hess-19-33-2015
- 538 Nguyen-Quang, T., Polcher, J., Ducharne, A., Arsouze, T., Zhou, X., Schneider, A.,  
 539 & Fita, L. (2018). ORCHIDEE-ROUTING: Revising the river routing scheme  
 540 using a high-resolution hydrological database. *Geoscientific Model Development*  
 541 *Discussions*, 11(12), 4965–4985. doi: 10.5194/gmd-11-4965-2018
- 542 Nicolle, P., Andréassian, V., Royer-Gaspard, P., Perrin, C., Thirel, G., Coron, L., &  
 543 Santos, L. (2021, September). Technical note: RAT – a robustness assessment  
 544 test for calibrated and uncalibrated hydrological models. *Hydrology and Earth*  
 545 *System Sciences*, 25(9), 5013–5027. doi: 10.5194/hess-25-5013-2021
- 546 Palmer, M. A., Reidy Liermann, C. A., Nilsson, C., Flörke, M., Alcamo, J., Lake,  
 547 P. S., & Bond, N. (2008). Climate change and the world’s river basins: Antic-  
 548 ipating management options. *Frontiers in Ecology and the Environment*, 6(2),  
 549 81–89. doi: 10.1890/060148
- 550 Perrin, C., Michel, C., & Andréassian, V. (2003, August). Improvement of a parsimonious  
 551 model for streamflow simulation. *Journal of Hydrology*, 279(1), 275–  
 552 289. doi: 10.1016/S0022-1694(03)00225-7
- 553 Polcher, J., Schrapffer, A., Dupont, E., Rinchiuso, L., Zhou, X., Boucher, O., ...  
 554 Servonnat, J. (2022, September). Hydrological modelling on atmospheric grids;  
 555 using graphs of sub-grid elements to transport energy and water. *EGUsphere*,  
 556 1–34. doi: 10.5194/egusphere-2022-690
- 557 Quintana-Seguí, P., Barella-Ortiz, A., Regueiro-Sanfiz, S., & Miguez-Macho, G.  
 558 (2020, May). The Utility of Land-Surface Model Simulations to Provide  
 559 Drought Information in a Water Management Context Using Global and Lo-  
 560 cal Forcing Datasets. *Water Resources Management*, 34(7), 2135–2156. doi:  
 561 10.1007/s11269-018-2160-9
- 562 Reaver, N. G. F., Kaplan, D. A., Klammler, H., & Jawitz, J. W. (2022, March).  
 563 Theoretical and empirical evidence against the Budyko catchment trajectory  
 564 conjecture. *Hydrology and Earth System Sciences*, 26(5), 1507–1525. doi:  
 565 10.5194/hess-26-1507-2022
- 566 Ribes, A., Thao, S., Vautard, R., Dubuisson, B., Somot, S., Colin, J., ... Soubey-  
 567 roux, J.-M. (2019, January). Observed increase in extreme daily rainfall  
 568 in the French Mediterranean. *Climate Dynamics*, 52(1), 1095–1114. doi:  
 569 10.1007/s00382-018-4179-2

- 570 Riedel, T., & Weber, T. K. D. (2020, September). Review: The influence of global  
571 change on Europe’s water cycle and groundwater recharge. *Hydrogeology Jour-*  
572 *nal*, 28(6), 1939–1959. doi: 10.1007/s10040-020-02165-3
- 573 Rottler, E., Francke, T., Bürger, G., & Bronstert, A. (2020, April). Long-  
574 term changes in central European river discharge for 1869–2016: Impact of  
575 changing snow covers, reservoir constructions and an intensified hydrolog-  
576 ical cycle. *Hydrology and Earth System Sciences*, 24(4), 1721–1740. doi:  
577 10.5194/hess-24-1721-2020
- 578 Rudolf, B., Beck, C., Grieser, J., Schneider, U., & Deutscher Wetterdienst, D.  
579 (2005). The Global Precipitation Climatology Centre (GPCP).
- 580 Schaner, N., Voisin, N., Nijssen, B., & Lettenmaier, D. P. (2012, September). The  
581 contribution of glacier melt to streamflow. *Environmental Research Letters*,  
582 7(3), 034029. doi: 10.1088/1748-9326/7/3/034029
- 583 Schneider, C., Laizé, C. L. R., Acreman, M. C., & Flörke, M. (2013, January). How  
584 will climate change modify river flow regimes in Europe? *Hydrology and Earth*  
585 *System Sciences*, 17(1), 325–339. doi: 10.5194/hess-17-325-2013
- 586 Siebert, S., Kummu, M., Porkka, M., Doell, P., Ramankutty, N., & Scanlon,  
587 B. (2015, March). A global data set of the extent of irrigated land from  
588 1900 to 2005. *Hydrology and Earth System Sciences*, 19, 1521–1545. doi:  
589 10.5194/hess-19-1521-2015
- 590 Stephens, G., Polcher, J., Zeng, X., van Oevelen, P., Poveda, G., Bosilovich, M.,  
591 ... Bony, S. (2023, January). The First 30 Years of GEWEX. *Bul-*  
592 *letin of the American Meteorological Society*, 104(1), E126-E157. doi:  
593 10.1175/BAMS-D-22-0061.1
- 594 Tafasca, S., Ducharne, A., & Valentin, C. (2020, July). Weak sensitivity of the  
595 terrestrial water budget to global soil texture maps in the ORCHIDEE land  
596 surface model. *Hydrology and Earth System Sciences*, 24(7), 3753–3774. doi:  
597 10.5194/hess-24-3753-2020
- 598 Vicente-Serrano, S. M., Peña-Gallardo, M., Hannaford, J., Murphy, C., Lorenzo-  
599 Lacruz, J., Dominguez-Castro, F., ... Vidal, J.-P. (2019). Climate, Irrigation,  
600 and Land Cover Change Explain Streamflow Trends in Countries Bordering  
601 the Northeast Atlantic. *Geophysical Research Letters*, 46(19), 10821–10833.  
602 doi: 10.1029/2019GL084084
- 603 Vincent, C., Fischer, A., Mayer, C., Bauder, A., Galos, S. P., Funk, M., ... Huss,  
604 M. (2017). Common climatic signal from glaciers in the European Alps  
605 over the last 50 years. *Geophysical Research Letters*, 44(3), 1376–1383. doi:  
606 10.1002/2016GL072094
- 607 Wang, F., Polcher, J., Peylin, P., & Bastrikov, V. (2018, July). Assimilation of  
608 river discharge in a land surface model to improve estimates of the continental  
609 water cycles. *Hydrology and Earth System Sciences*, 22(7), 3863–3882. doi:  
610 10.5194/hess-22-3863-2018
- 611 Wang, W., Zhang, Y., & Tang, Q. (2020, December). Impact assessment of climate  
612 change and human activities on streamflow signatures in the Yellow River  
613 Basin using the Budyko hypothesis and derived differential equation. *Journal*  
614 *of Hydrology*, 591, 125460. doi: 10.1016/j.jhydrol.2020.125460
- 615 Weedon, G. P., Balsamo, G., Bellouin, N., Gomes, S., Best, M. J., & Viterbo, P.  
616 (2014). The WFDEI meteorological forcing data set: WATCH Forcing Data  
617 methodology applied to ERA-Interim reanalysis data. *Water Resources Re-*  
618 *search*, 50(9), 7505–7514. doi: 10.1002/2014WR015638
- 619 Xiong, M., Huang, C.-S., & Yang, T. (2020, June). Assessing the Impacts of Climate  
620 Change and Land Use/Cover Change on Runoff Based on Improved Budyko  
621 Framework Models Considering Arbitrary Partition of the Impacts. *Water*,  
622 12(6), 1612. doi: 10.3390/w12061612
- 623 Zanardo, S., Harman, C. J., Troch, P. A., Rao, P. S. C., & Sivapalan, M. (2012).  
624 Intra-annual rainfall variability control on interannual variability of catchment

- 625 water balance: A stochastic analysis. *Water Resources Research*, 48(6). doi:  
626 10.1029/2010WR009869
- 627 Zhang, L., Hickel, K., Dawes, W. R., Chiew, F. H. S., Western, A. W., & Briggs,  
628 P. R. (2004). A rational function approach for estimating mean annual  
629 evapotranspiration. *Water Resources Research*, 40(2). doi: 10.1029/  
630 2003WR002710
- 631 Zhang, L., Potter, N., Hickel, K., Zhang, Y., & Shao, Q. (2008, October). Water  
632 balance modeling over variable time scales based on the Budyko framework –  
633 Model development and testing. *Journal of Hydrology*, 360(1), 117–131. doi:  
634 10.1016/j.jhydrol.2008.07.021
- 635 Zhao, J., Huang, S., Huang, Q., Wang, H., & Leng, G. (2018, September). De-  
636 tecting the Dominant Cause of Streamflow Decline in the Loess Plateau  
637 of China Based on the Latest Budyko Equation. *Water*, 10(9), 1277. doi:  
638 10.3390/w10091277
- 639 Zhao, W., & Li, A. (2015, August). A Review on Land Surface Processes Modelling  
640 over Complex Terrain. *Advances in Meteorology*, 2015, e607181. doi: 10.1155/  
641 2015/607181
- 642 Zheng, Y., Huang, Y., Zhou, S., Wang, K., & Wang, G. (2018, December). Ef-  
643 fect partition of climate and catchment changes on runoff variation at the  
644 headwater region of the Yellow River based on the Budyko complemen-  
645 tary relationship. *Science of The Total Environment*, 643, 1166–1177. doi:  
646 10.1016/j.scitotenv.2018.06.195
- 647 Zveryaev, I. I. (2004). Seasonality in precipitation variability over Europe. *Journal*  
648 *of Geophysical Research: Atmospheres*, 109(D5). doi: 10.1029/2003JD003668

1 **Identifying and quantifying the impact of climatic and**  
2 **non-climatic drivers on river discharge in Europe**

3 **Julie Collignan<sup>1</sup>, Jan Polcher<sup>1</sup>, Sophie Bastin<sup>2</sup>, Pere Quintana-Segui<sup>3</sup>**

4 <sup>1</sup>Laboratoire de Météorologie Dynamique/IPSL - Ecole Polytechnique/CNRS -, Paris, France

5 <sup>2</sup>Laboratoire Atmosphères, Observations Spatiales/IPSL - CNRS -, Paris, France

6 <sup>3</sup>Observatori de l'Ebre (Universitat Ramon Llull – CSIC), Roquetes, Spain

7 **Key Points:**

- 8 • Attribution of streamflow trends to climate drivers  
9 • Larger effect on streamflow of non-climatic drivers  
10 • Strong impact of human activities, especially over Spain

---

Corresponding author: Julie Collignan, [julie.collignan@lmd.ipsl.fr](mailto:julie.collignan@lmd.ipsl.fr)

## Abstract

Our water resources have changed over the last century through a combination of water management evolutions and climate change. Understanding and decomposing these drivers of discharge changes is essential to preparing and planning adaptive strategies. We propose a methodology combining a physical-based model to reproduce the natural behavior of river catchments and a parsimonious model to serve as a framework of interpretation, comparing the physical-based model outputs to observations of discharge trends. We show that over Europe, especially in the South, the dominant explanations for discharge trends are non-climatic factors. Still, in some catchments of Northern Europe, climate change seems to be the dominating driver of change. We hypothesize that the dominating non-climatic factors are irrigation development, groundwater pumping and other human water usage, which need to be taken into account in physical-based models to understand the main drivers of discharge and project future changes.

## Plain Language Summary

Water is an essential resource. Its access and management are key challenges in the context of climate change. Changes in precipitation distribution and intensity and other climate effects lead to a change in the water availability and in the discharge of rivers. On top of that, humans intervene to uptake water from rivers and change streamflow dynamics. To better assess management practices and prepare for future climate conditions, it is important to understand which part of discharge evolution is due to climate and which part is due to human intervention. In this article, we present an innovative methodology to do so. We show that over Europe, if discharge in the North is mostly impacted by the evolution of climate, in the rest, water management practices are the main cause of discharge changes. This is especially the case for the drying discharge trends in the South. Therefore, the evolution of management practices must be particularly of interest when constructing adaptation pathways to future climate conditions.

## 1 Introduction

Water is an essential resource for both ecosystems and human needs. Floods or water scarcity can lead to environmental catastrophes, conflicts and economic hardships. Understanding the evolution of water availability is a key challenge in the context of climate change and a highly managed continental water cycle. To study the evolution of water resources, one key variable is streamflow. Being at the surface, it is directly related to freshwater available to humans and ecosystems (Dai, 2016). In order to optimize its availability and reduce the impacts of floods and hydrological droughts, mankind has managed it over the last millennia. Because of its central role in our water resources, it has also been well observed over the last century.

From a geophysical perspective, streamflow provides a comprehensive overview of the water dynamics of catchments as it is the result of the catchment-integrated balance between water storage, precipitation and evapotranspiration (Milly et al., 2005; Rottler et al., 2020). These last two fluxes are dominated by climate processes and thus driven by atmospheric variability and trends (Christidis & Stott, 2022; García-Ruiz et al., 2011). On the other hand, it is through the management of water storage (reservoirs or groundwater pumping) and evaporation (land use and irrigation) that humans optimize the benefits they take from surface water and modify streamflows (Schneider et al., 2013; Riedel & Weber, 2020).

All of these processes have confounding effects on river discharge, which makes it difficult to detect and attribute trends in water resources (Rottler et al., 2020; Ficklin et al., 2018). With climate change, precipitation distribution, frequency and intensity are evolving, along with an increase in atmospheric water demand due to increased en-

60 ergy available at the surface and atmospheric water holding capacity and to changes in  
61 turbulences (Douveille et al., 2021; Christidis & Stott, 2022; García-Ruiz et al., 2011; Ribes  
62 et al., 2019; Dezsi et al., 2018). In turn, human activities and management, through ab-  
63 stractions (for irrigation, domestic uses...) and regulations (dams, reservoirs...), directly  
64 impact the partitioning of water between runoff and evapotranspiration along with flow  
65 seasonality, due to additional water uptakes and to controlled water releases (Rottler et  
66 al., 2020; García-Ruiz et al., 2011; Ficklin et al., 2018). Therefore, streamflow changes  
67 are driven by climate change and anthropogenic activities, both influencing catchment  
68 dynamics and equilibrium.

69 To project future streamflow changes and adapt water management strategies to  
70 climate change, it is essential first to understand the relative weight of these different  
71 drivers in streamflow dynamics. Being able to attribute past changes in river discharge  
72 to either climatic factors or human intervention on the land surface processes provides  
73 invaluable information to water managers in an evolving water cycle.

74 Physical-based land surface models (LSMs) and global hydrological models (GHMs)  
75 have been developed to understand streamflow dynamics, reproduce land surface pro-  
76 cesses and predict the evolution of the water cycle using different scenarios for the fu-  
77 ture (W. Zhao & Li, 2015; Nazemi & Wheeler, 2015). They have grown more complex  
78 over time and represent, at best, the current understanding of surface/atmosphere in-  
79 teractions, vegetation dynamics and hydrological processes under the control of climate  
80 (Tafasca et al., 2020; Quintana-Seguí et al., 2020; Stephens et al., 2023). These models  
81 are very useful to study patterns of change and trends and link them to specific processes  
82 (Douveille et al., 2021; Zanardo et al., 2012; Alkama et al., 2010; Do et al., 2020). How-  
83 ever, to this day, they fail to effectively include most anthropogenic water usage and man-  
84 agement, even if progress is being made in that direction (F. Wang et al., 2018; Nazemi  
85 & Wheeler, 2015).

86 In view of the complexity of land surface processes and the lack of data, another  
87 class of models has also been developed: parsimonious or calibrated models. Based on  
88 the perceived functioning of the surface hydrology (Beven & Chappell, 2021), relations  
89 and parameters are selected and then adjusted over a period to represent, at best, ac-  
90 tual streamflow characteristics. These models have demonstrated their value for oper-  
91 ational short-term predictions and to represent and detect current trends in discharge  
92 with a simplified interpretation tool (Jiang et al., 2015; Andréassian et al., 2016; Per-  
93 rin et al., 2003). However, they are limited in their ability to predict changes associated  
94 with specific drivers due to the difficulty of physical interpretation of the adjusted pa-  
95 rameters and the undetermined sensitivity of these parameters to the drivers (Zheng et  
96 al., 2018; Andréassian et al., 2016; Coron et al., 2014; Nicolle et al., 2021). Still they have  
97 been used to try and separate the effect of anthropogenic activities from climatic drivers,  
98 often comparing a reference "untouched" period or area to a post-change period or to  
99 a similar but highly anthropized area (Ficklin et al., 2018; W. Wang et al., 2020; Palmer  
100 et al., 2008; Ahn & Merwade, 2014; Zheng et al., 2018; Luo et al., 2020; J. Zhao et al.,  
101 2018). However, these methods all rely on the debatable assumption that the adjusted  
102 parameters are independent of climate variability (Coron et al., 2014; Andréassian et al.,  
103 2016; Reaver et al., 2022).

104 Using both classes of models, we propose a method to analyze observed annual river  
105 discharge and decompose observed trends into climate-driven changes and those caused  
106 by human intervention on the continental water cycle. The LSM is chosen as the climatic  
107 reference as it represents the behavior of catchments and land surface dynamics, respond-  
108 ing to changes in climate variables only. Due to the incomplete representation of the com-  
109 plex land surface processes and the lack of representation of human water management,  
110 the direct validation of the predicted river discharge to observation is difficult (Hagemann  
111 & Dümenil, 1997). The Budyko space and the one-parameter parsimonious model pro-  
112 posed by Fu's equation (Zhang et al., 2004) is used as a framework for interpreting both

113 the LSM’s simulated and the observed historical discharge. This parsimonious model in-  
 114 troduces a parameter allowing to isolate the partial trends in discharge ( $Q$ ) due to a change  
 115 in catchment evaporation efficiency from the partial trend due to changes in the two main  
 116 average climate variables precipitation ( $P$ ) and potential evapotranspiration ( $PET$ ) (Collignan,  
 117 Polcher, Bastin, & Quintana-Segui, 2023). Projecting the LSM output onto this frame-  
 118 work allows to derive the climate sensitivity of the adjusted parameter of the parsimo-  
 119 nious model. In turn, comparing these results to the interpretation of observed histor-  
 120 ical records by the Budyko model allows to isolate the trends due to changes in evap-  
 121 oration efficiency and land characteristics not represented by the LSM. This separates  
 122 the observed changes in streamflow into a component that can be attributed to climate  
 123 variations and another that can be linked to human activities.

## 124 2 Method

125 The Budyko framework is a relatively simple empirical framework which relies on  
 126 balancing the water and energy fluxes through only a few variables (precipitations  $P$  and  
 127 potential evapotranspiration  $PET$ ) to express the partitioning of water between evap-  
 128 otranspiration  $E$  and runoff. As opposed to other simple empirical models such as lin-  
 129 ear regression models, it accounts for physical boundaries: the water limit and the en-  
 130 ergy limit on the system. For the framework to work, it needs to be applied to a closed  
 131 system where the boundaries can be defined, such as a watersheds at an equilibrium state  
 132 (the variations of water storage within the catchment are supposed to be small). It is  
 133 simple enough to be applicable to a wide variety of observed catchments as only basic  
 134 variables are needed. In this study we used the parametric equation of Fu-Tixeront (Zhang  
 135 et al., 2004) (Zhang et al., 2008) (Zheng et al., 2018). It reduces for each catchment its  
 136 evaporation efficiency to a single specific parameter  $\omega$  (Equ. 1), fitted over hydrologi-  
 137 cal year averages, in a given period. For the same climatic conditions  $P$ ,  $PET$ , a catch-  
 138 ment with a higher  $\omega$  will evaporate more than another one with a smaller  $\omega$ .

139 In the original framework, this parameter is assumed to be constant since the wa-  
 140 tershed is considered to be in a stationary state and only driven by climate.

$$\frac{E}{P} = 1 + \frac{PET}{P} - \left( 1 + \left( \frac{PET}{P} \right)^\omega \right)^{\frac{1}{\omega}} \quad (1)$$

141  $E$  is the actual evaporation at the scale of the catchment. With the same assump-  
 142 tion of a closed system and no water storage change, the water continuity yields for dis-  
 143 charge  $Q = P - E$ .

144 Here, we consider only that the system is piece-wise stationary and that the pa-  
 145 rameter can be assumed to the constant over a short period (11 years) (Han et al., 2020).  
 146 This introduces a time-dependence in the parameter  $\omega$  by successive fits over an 11-year  
 147 time-moving window. We therefore capture the long-term effects of climate change and  
 148 anthropogenic activities, both influencing catchments responses.

149 As a result, both the annual mean of  $P$  and  $PET$ , regrouped in the variable  $C$  later  
 150 on, and for the evaporation efficiency  $\omega$  are time dependent. This allows to construct a  
 151 framework of interpretation, with a simple decomposition of discharge trends  $Q$ : a par-  
 152 tial trends due to long-term changes in average climate variable and a partial trend due  
 153 to changes in catchment responses. More details for this methodology are given in (Collignan,  
 154 Polcher, Bastin, & Quintana-Segui, 2023). In this framework, the anthropogenic water  
 155 management and water usage will only change the catchment responses and not the cli-  
 156 mate variables.

157 By applying the method to the observed catchments and the representation of these  
 158 catchments in a land surface model, the relative contribution of climate to trends in dis-  
 159 charge can be quantified. The two systems considered are :

- 160 • **A climate-driven system, referred as climatic system:** An LSM is used to  
 161 estimate the climate induced changes in the evaporation efficiency ( $\omega_c$ ). The LSM  
 162 stands as our climatic reference. It provides us with the following information:
  - 163 –  $\Delta Q_{climat}(C, \omega_c)$ : defined as the climate driven discharge trends.
  - 164 –  $\Delta Q_c(C, \overline{\omega_c})$ : partial trend due to fluctuations in annual averages of climate vari-  
 165 ables ( $C$ ), where  $\overline{\omega_c}$  is the average evaporation efficiency over the entire period.
  - 166 –  $\Delta Q_c(C_{rand}, \omega_c)$ : partial trend due to climatic impact on evaporation efficiency  
 167  $\omega_c$ , where  $C_{rand}$  is a random climate with no trends.
- 168 • **The observation-based system, referred as actual system:** the framework  
 169 is used to decompose the observed discharge changes. We successively fit the frame-  
 170 work to discharge observations, getting another time series of the evaporation ef-  
 171 ficiency parameter  $\omega_a$ . This provides the following information:
  - 172 –  $\Delta Q_{actual}(C, \omega_a)$ : overall trend in  $Q$  in the actual system.
  - 173 –  $\Delta Q_a(C, \overline{\omega_a})$ : partial trend due to changes in  $C$ .
  - 174 –  $\Delta Q_a(C_{rand}, \omega_a)$ : By randomizing the climate, the partial trend due to the evo-  
 175 lution of evaporation efficiency  $\omega_a$  can be estimated. In that case, all changes  
 176 in the watershed characteristics (anthropogenic as well as its climate in-  
 177 duced) are considered.

178 We illustrate the differences in both systems over a given catchment, with a fig-  
 179 ure of  $Q_{climat}$ ,  $Q_{actual}$ ,  $\omega_c$  and  $\omega_a$ , for the station of Castejon, upstream of the Ebro river  
 180 in Spain (in supplementary materials, Fig. S3).

181 We consider that the LSM accurately reproduces dynamic changes in an idealized  
 182 natural catchment driven by observed climatic conditions, even if it might have biases  
 183 in the absolute values of discharge. Therefore we only compare trends between both sys-  
 184 tems. All trends are computed using the Mann-Kendall non-parametric test, associated  
 185 with the Thiel-Sen slope estimator (Xiong et al., 2020), with a 0.05 p-value threshold  
 186 for significance.

## 187 3 Data

### 188 3.1 The Land Surface Model ORCHIDEE

189 The LSM used in this study is the Organizing Carbon and Hydrology In Dynamic  
 190 Ecosystems (ORCHIDEE) (Krinner et al., 2005) from the Institut Pierre Simon Laplace  
 191 (IPSL). The current version of the model simulates the global carbon cycle and quan-  
 192 tifies terrestrial water and energy balance through biophysical and natural biogeochem-  
 193 ical processes. It can include some anthropogenic interference such as land cover changes,  
 194 forest and grassland management or irrigation (Guimberteau et al., 2012). Here the model  
 195 is used without these options, as only the climatic dependences of hydrology are sought.  
 196 Used in off-line conditions, the atmospheric conditions are forced by a given data-set.

### 197 3.2 Forcing datasets

198 Three different climatic datasets are used to drive the LSM. These datasets are used  
 199 as input to the off-line LSM and provide the variables needed in Fu's equation 1. The  
 200 main one is the forcing dataset GSWP3 (Hyungjun, 2017), covering the 1901-2012 pe-  
 201 riod at a 3-hourly resolution with a geographic resolution of  $0.5^\circ \times 0.5^\circ$ . It is a dynam-  
 202 ical downscaling of 20th Century Reanalysis using a Global Spectral Model. It is bias-  
 203 corrected using Global Precipitation Climatology Center (GPCC) (Rudolf et al., 2005)  
 204 and Climate Research Unit (CRU) observational data (Harris et al., 2020). The results  
 205 presented later on are obtained with this forcing dataset.

We also use two other forcings, WFDEI-GPCC (Weedon et al., 2014) and E2OFD (Beck et al., 2017), both covering the 1979 to 2014 period. Testing the methodology with different independent climate datasets allows to verify the robustness of our results comparing the two systems and their sensitivity to the choice of climate forcing used (see supplementary materials).

### 3.3 Watersheds and discharge observation datasets

The river discharge observations collected by the Global Runoff Data Center (GRDC) from gauging stations all over Europe (GRDC, 2020) are the base of the current study. They were completed over Spain with data obtained from the Geoportail of Spain Ministerio (Ministerio para la Transición Ecológica y el Reto Demográfico, 2020) and over France with data from the database HYDRO (Ministere de l'ecologie, du developpement durable et de l'energie, 2021).. In the final analysis, only 814 stations were kept with at least 50 years of observations and for which we were able to satisfyingly reproduce the upstream catchment in the hydrological routing of the LSM (Polcher et al., 2022; Nguyen-Quang et al., 2018), based on the dataset HydroSHEDS (Hydrological Data and Maps Based on Shuttle Elevation Derivatives at Multiple Scales) (Lehner et al., 2008).

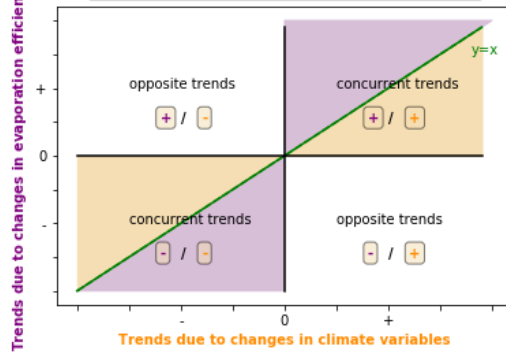
## 4 Results

### 4.1 Decomposing the trends in river discharge over the past century

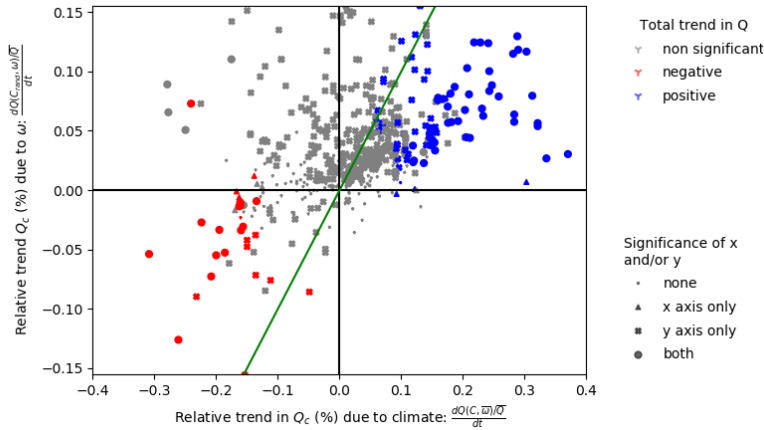
The framework defined by the parsimonious model chosen allows to separate trends in river discharge ( $Q$ ) into the part explained by the evolution of climate  $C$  (x-axis) and a partial trend due to changes in the catchment affecting evaporation efficiency ( $\omega$ ) (y-axis). Figure 1a allows to illustrate the relative importance of both components of the trends as estimated with the methodology presented above, using a 100-year-long simulation with an LSM and the observed discharge at 569 gauging stations.

Positioning the results for one catchment in Fig. 1a allows to illustrate the magnitudes of the partial trends due to each component and whether they are concurrent or opposite and if they tend to increase or decrease discharge. Two different systems are projected on this framework for comparison (see Method): the climatic system ( $Q_{climat}$ ) based on the LSM outputs and the actual system ( $Q_{actual}$ ) based on observed records.

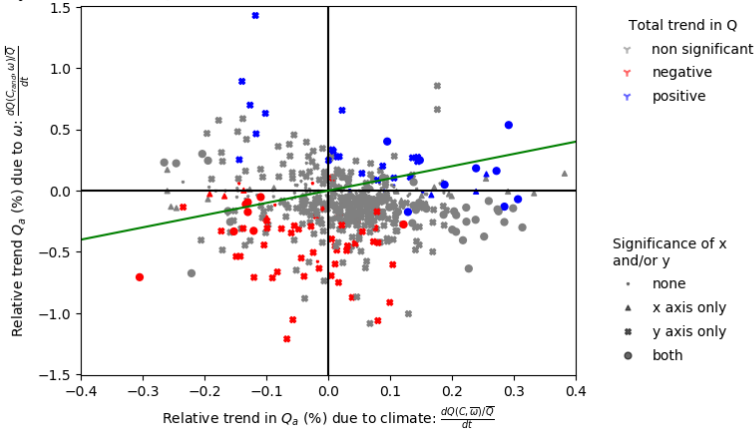
Our results show that in the case of the climatic system (Fig. 1b), the changes in annual mean climate variables have about a four times larger impact than the changes in evaporation efficiency on relative annual mean discharge trends. Overall, almost all catchments where  $Q_{climat}$  has significantly changed (catchments with significant trends correspond to colored points) have concurrent trends in both components. A high covariance between these two components allows to better detect the trends. More generally, there is a dominance of the trends in annual mean in climate variables  $P$ ,  $PET$ , amplified by the response of evaporation efficiency of the catchment induced by climate change. These cases correspond to catchments where an increase in  $P$  and/or a decrease in  $PET$  tends to increase annual mean discharge or inversely for a decrease. For instance, if an increase in  $P$  is inhomogeneous, with an even stronger increase in winter precipitation, the partitioning towards runoff is usually higher, which translates into a decreased evaporation efficiency and thus an even stronger increase of  $Q_{climat}$  (top right quadrant, Fig. 1b). Therefore in this example, the increase in the annual mean  $Q_{climat}$  is not only due to an increase in annual mean  $P$  but is amplified by the more contrasted seasonality and its impact on evaporation efficiency. More generally, there are fewer catchments where the changes in the evaporation efficiency tend to decrease discharge in the climatic system, except when they concur with a high decrease in relative discharge due to a decrease in  $P$  and/or an increase in  $PET$ . This is coherent with the increasing intensity and contrasted seasonality of precipitation events observed over Europe (Christidis &



(a) Interpretation scheme: comparing significant trends due to climate variables or due to  $\omega$ . The graphs have four quadrants: the top right and the bottom left ones correspond to area of the graph where the climatic trend and the area due to  $\omega$  are complementary/ going into the same direction. The top left one contains the basins for which the trends due to  $\omega$  are positive and the trends due to climate variables are negative and the bottom right quadrant the opposite.



(b) Climatic system  $Q_{climat}$ : relative trends (%/yr over the century) due to changes in  $\omega_c$  versus relative trends due to changes in climate variables  $C$



(c) Actual system  $Q_{actual}$ : relative trends (%/yr over the century) due to changes in  $\omega_a$  versus relative trends due to changes in climate variables  $C$

**Figure 1.** Comparing the relative trends ( $\frac{dQ}{dt}/\bar{Q}$ ) due to a change in climate variables or due to a change in evaporation efficiency  $\omega$  in the evolution of discharge, for both system  $Q_{climat}$  and  $Q_{actual}$ . One point corresponds to a basin with at least 50 years of river discharge observations over Europe. The scale of trends due to  $\omega_a$  in the actual system is ten times larger than the one for trends due to  $\omega_c$  in the climatic system. The green line is the line  $y = x$ . The color scale represents the significance of the trend in  $Q$  when all factors are considered. The markers indicate whether the partial trends are significant due to changes in  $C$  (x-axis), in  $\omega$  (y-axis), or both.

255 Stott, 2022; Riedel & Weber, 2020; Zveryaev, 2004; Ribes et al., 2019; Douville et al.,  
 256 2021), which would logically tend to decrease evaporation efficiency by increasing local  
 257 runoff, and therefore lead to a positive partial trend in discharge.

258 In the case of the observed system (Fig. 1c), the relationship between the two partial  
 259 trends looks very different. The one linked to changes in evaporation efficiency is larger  
 260 than the partial trends linked to the annual mean in  $P$  and  $PET$  by a factor of 3. More  
 261 generally, the total trends in  $Q_{actual}$  (catchments with significant trends correspond to  
 262 colored points) follow the partial trends due to changes in the catchments' evaporation  
 263 efficiency. Therefore, in the actual system, the trends in discharge are mainly due to changes  
 264 in catchment behavior due to non-climatic factors. Contrary to when only climate change  
 265 is considered for natural catchments, land use changes and human water management  
 266 tend to increase the evaporation efficiency of catchments and, therefore, decrease  $Q_{actual}$ .  
 267 This is coherent with activities such as irrigation, or agriculture in general, which aim  
 268 at optimizing the evapotranspiration over catchments.

## 269 4.2 Geographical distribution of discharge trend characteristics

270 The spatial distribution of the significant relative trends (Fig. 2) is spatially coher-  
 271 ent, which also attests to the method's robustness. When some specific catchments  
 272 are referred to, the geographic location of these catchments is illustrated in supplement-  
 273 ary material (Fig. S2).

274 In the climatic system (Fig. 2a), basins in eastern Europe and Spain are getting  
 275 dryer with trends in discharge between  $-0.2\%/yr$  and  $-0.5\%/yr$  over the past century. In  
 276 central and northern Europe, the climatic discharge is increasing with trends of  $+0.2\%/yr$   
 277 to  $0.5\%/yr$  over the past century. Similarly to the previous results, we observe that in  
 278 this system, the trends in discharge  $Q_{climat}$  (Fig. 2a) are mostly driven by changes in  
 279 average climate variables  $C$  (Fig. 2c) and not to changes in evaporation efficiency  $\omega_c$  (Fig.  
 280 2e). These partial trends due to changes in the evaporation efficiency  $\omega_c$  (Fig. 2e) are  
 281 small (between  $-0.2\%/yr$  to  $+0.2\%/yr$ ) and are mostly positive. Their effect is negligi-  
 282 ble when looking at the total trends in discharge (Fig. 2a). It can however amplify the  
 283 partial trend due to changes in the annual average of climate variables  $C$ . It corresponds  
 284 to the top-right and bottom-left quadrants in Fig. 1b. This effect is illustrated in the  
 285 Duero basin in north-western Spain, where both partial trends concur to a decrease in  
 286  $Q_{climat}$ . They can also cancel each other out, for instance, in the Tiber River in Italy,  
 287 where the decrease in  $Q_{climat}$  due to changes in  $C$  is not significant in the overall changes  
 288 in  $Q_{climat}$ .

289 Again, for the actual system, our results show that the discharge trends (Fig. 2b)  
 290 are mostly explained by changes in the evaporation efficiencies (Fig. 2f). Here the changes  
 291 in the evaporation efficiency  $\omega_a$  encompass all changes in the catchment's evaporative  
 292 behaviors, those induced by climate and those by changing water usage. Similarly to re-  
 293 sults from other studies (Vicente-Serrano et al., 2019) over Western Europe, we find the  
 294 highest negative trends are over Southern Spain and are mostly driven by non-climatic  
 295 factors. To facilitate the comparison, scales of the Fig. 2 are fixed thus for Fig. 2d and  
 296 Fig. 2f they saturate, not showing that the trends are a lot higher in Spain, with up to  
 297  $-4.4\%/yr$  change over the past century in  $Q_{actual}$ . Over the rest of Europe, trends are  
 298 lower and less significant, with positive trends generally in northern Europe, Great Britain  
 299 and Sweden and negative trends over central Europe. The south of Spain corresponds  
 300 to an area where both climate changes and changes related to human activities led to  
 301 a significant decrease in river discharge over the past century. There, mainly, the changes  
 302 in evaporation efficiency result in decreasing trends in  $Q_{actual}$  (Fig. 2f). This is coher-  
 303 ent with increasing irrigation water uptakes. However, the Guadiana River stands out  
 304 in our results. It seems that over that specific catchment, the overall effect of human wa-  
 305 ter management and land use changes tend to increase  $Q_{actual}$ , contrary to the rest of

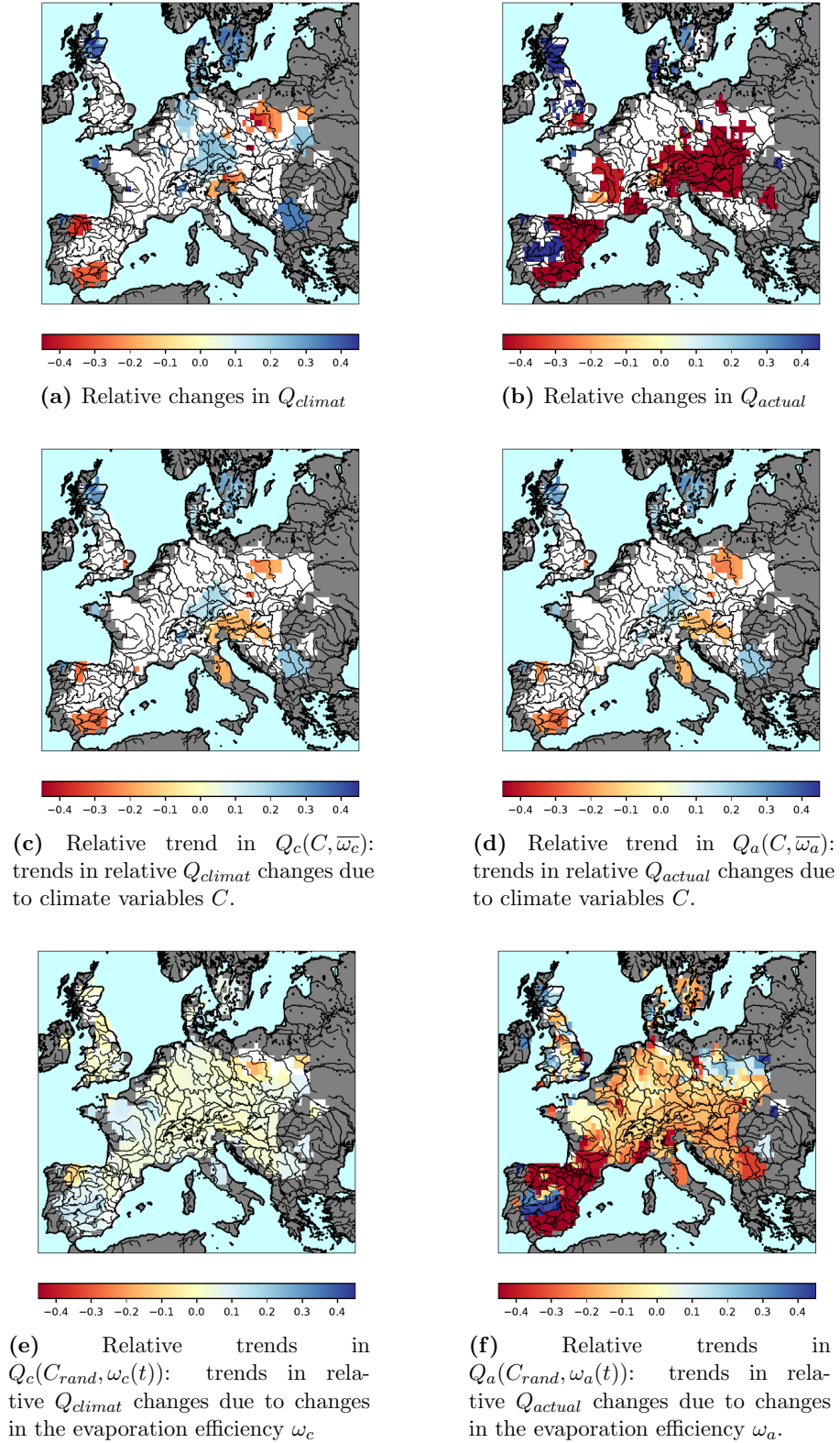


**Figure 2.** Significant trends in the relative river discharge  $Q/\bar{Q}$  over the time period 1901-2012 (%/yr over the century). The scales have been forced to be the same for all maps for comparison purposes but the extrema can go higher or lower.

Spain. As discussed later, this could be linked to unsustainable groundwater pumping (Holtz & Pahl-Wostl, 2012), which invalidates the hypothesis of no water storage change and, therefore, results in a lower apparent evaporation efficiency and an artificially underestimated evapotranspiration, increasing the resulting discharge. More generally, there are several basins over Europe where the trends induced by changes in the evaporation efficiency lose their significance when the climate variability is considered in the reconstructed discharge. See, for instance, western France, northern Germany, Serbia.

Interestingly, when we draw similar maps for sub-periods of 10 years, the impact of evaporation efficiency changes on discharge is not dominant anymore. At the decadal scale, the climatic variability is high. This climatic noise covers the effect of changes in the catchment's evaporation efficiency in discharge trends. At the scale of the century, the signal-to-noise ratio is higher, bringing to light the long-term role of changes in the catchment's evaporation efficiency and catchment's behavior on discharge.

## 5 Discussion

Our method uses a parsimonious hydrological model to decompose the observed river discharge trends into climate-driven processes, as estimated with a state-of-the-art LSM, and non-climatic changes that can be attributed to human activities. It can be generalized to the use of any couple of calibrated parsimonious model and physical-based model and be an effective operational tool to estimate and illustrate the effect of non-climatic drivers and land surface changes not well accounted for in current models and which may have a strong direct impact on water resources.

We show that the dominant explanation for river discharge trends is non-climatic factors, especially in Southern Europe. In some catchments of Northern Europe, climate change seems to be the dominating driver of change. Still, in accordance with previous studies (Gudmundsson et al., 2017), our results highlight the fact that not accounting for non-climatic trends leads to high under-estimation of discharge changes in the physical-based model used and therefore to high uncertainties in projections of future water resource trends, especially when looking at long-term trends.

With this methodology, we can only estimate the magnitude of non-climatic trends but not attribute them to specific processes. In some areas where a dominant process can be hypothesized, such as irrigation, correlation with indicators can allow to verify the plausibility of the assumed cause. For instance, over Spain, especially over the Ebro basin, the strong increase in evaporation efficiency and reduced discharge is correlated to the development of dams with a coefficient above 0.7 when correlating  $\omega_a$  to reservoirs levels for 6 sub-basins in this catchment. Dams water storage is an indicator for human management of water resources impacting the evaporation efficiency of watersheds. More generally, we see that the changes in the evaporation efficiency intensified over the second part of the century, where areas equipped for irrigation have been developed (Angelakis et al., 2020; Siebert et al., 2015). However, the available data are insufficient to attest to a correlation with that latter factor or with the effective amount of water used for irrigation. Groundwater pumping and glacier melt can explain positive trends in discharge due to additional sources of water not accounted for in the climatic system, which lead to artificially low evaporation efficiencies in our framework. For the Guadiana River in Spain, the unsustainable groundwater pumping (Holtz & Pahl-Wostl, 2012; Llamas et al., 2015; Esteban & Albiac, 2012) can explain the positive trend. In a similar way, for the Po river in Italy, which is highly irrigated (Siebert et al., 2015), we would expect a strong decrease in discharge as in most of Spain, but glacier melt brings additional water to the system (Schaner et al., 2012; Vincent et al., 2017; Huss & Hock, 2018), explaining a reduced detected negative trend over the end of the century. Other phenomena, such as soil sealing and river management, would be expected to have similar effects due to a decrease in evapotranspiration or to an artificial enhancement of runoff.

357 Changes in land use as represented in ORCHIDEE (Lawrence et al., 2016) are shown  
 358 to have little effect on discharge over the studied period and area but could have a more  
 359 significant effect at finer scale over small catchments.

360 Quantifying the contribution of climatic and non-climatic factors to changes in river  
 361 discharge is an important first step. But it should be followed by an attribution. The  
 362 use of the LSM in its current state allows to attribute the changes due to climate. How-  
 363 ever, the non-climatic factors remain challenging to attribute to specific processes, es-  
 364 pecially since most factors have concurring and competing effects. Detection and attri-  
 365 bution methods have been developed in climate studies to assess anthropogenic climate  
 366 change. They have allowed to determine the role of different factors by reproducing them  
 367 first in GCMs (Hegerl & Zwiers, 2011; Douville et al., 2021). Similarly, we would need  
 368 to simulate water usage such as irrigation, dam management, groundwater pumping and  
 369 other missing phenomena such as glacier melting in the LSMs so that their impact on  
 370 the evaporation efficiency can be identified and their contribution to the non-climatic  
 371 trend quantified.

372 Understanding and quantifying the contribution of various processes contributing  
 373 to observed discharge changes over the past century is an essential step in developing adap-  
 374 tation strategies to face climate change. In the future, changes in climatic variables are  
 375 expected to increase even further, with increase in intense precipitation events (Ribes  
 376 et al., 2019; Douville et al., 2021), an increase in evaporative demand and especially a  
 377 decrease in average precipitation leading to water scarcity over southern Mediterranean  
 378 Europe (Gudmundsson et al., 2017; Alkama et al., 2013). Concurrently, in Europe, hu-  
 379 man water management is expected to evolve to adapt to climate change and other con-  
 380 straints, such as changes in water and energy demand and regulations (Arheimer et al.,  
 381 2017). For instance, the extent of irrigated land in Europe peaked at the end of the 20th  
 382 century and the future irrigation evolution is expected to follow new goals and mostly  
 383 rely on improved efficiency (Adeyeri et al., 2020). Therefore, the balance between the  
 384 different terms influencing catchment evaporation efficiency and discharge may change.  
 385 If non-climatic factors dominated over the past century to explain discharge trends, it  
 386 may not be the same in the future. Attribution needs to be tested over the documented  
 387 past to improve the representation of non-climatic processes and allow the effective pro-  
 388 jection of future evolutions and eventual changes in this balance.

## 389 Open Research Section

390 The outputs of the LSM ORCHIDEE for each catchment used in this study with  
 391 the forcing GSWP3 are gathered in a file freely available on Zenodo.org (Collignan, Polcher,  
 392 Bastin, & Quintana-Seguí, 2023). This file also contains the description of the stations  
 393 used in the study: their location, the size of the upstream area used to position the sta-  
 394 tion on the grid and annual averages of streamflow observations.

## 395 Acknowledgments

396 We would like to acknowledge the support of the Agence Nationale de la Recherche un-  
 397 der contract HLIaise (ANR-19-CE01-0017-02). The lead author would like to thank  
 398 Institut Polytechnique de Paris for the Gaspard Monge fellowship, which funded her PhD  
 399 thesis.

## 400 References

- 401 Adeyeri, O. E., Laux, P., Lawin, A. E., & Arnault, J. (2020, March). Assessing  
 402 the impact of human activities and rainfall variability on the river discharge  
 403 of Komadugu-Yobe Basin, Lake Chad Area. *Environmental Earth Sciences*,  
 404 79(6), 143. doi: 10.1007/s12665-020-8875-y

- 405 Ahn, K.-H., & Merwade, V. (2014, July). Quantifying the relative impact of climate  
406 and human activities on streamflow. *Journal of Hydrology*, *515*, 257–266. doi:  
407 10.1016/j.jhydrol.2014.04.062
- 408 Alkama, R., Kageyama, M., & Ramstein, G. (2010). Relative contributions of  
409 climate change, stomatal closure, and leaf area index changes to 20th and  
410 21st century runoff change: A modelling approach using the Organizing  
411 Carbon and Hydrology in Dynamic Ecosystems (ORCHIDEE) land surface  
412 model. *Journal of Geophysical Research: Atmospheres*, *115*(D17). doi:  
413 10.1029/2009JD013408
- 414 Alkama, R., Marchand, L., Ribes, A., & Decharme, B. (2013, July). Detec-  
415 tion of global runoff changes: Results from observations and CMIP5 ex-  
416 periments. *Hydrology and Earth System Sciences*, *17*(7), 2967–2979. doi:  
417 10.5194/hess-17-2967-2013
- 418 Andréassian, V., Coron, L., Lerat, J., & Le Moine, N. (2016, November). Climate  
419 elasticity of streamflow revisited – an elasticity index based on long-term hy-  
420 drometeorological records. *Hydrology and Earth System Sciences*, *20*(11),  
421 4503–4524. doi: 10.5194/hess-20-4503-2016
- 422 Angelakis, A. N., Zaccaria, D., Krasilnikoff, J., Salgot, M., Bazza, M., Roccaro, P.,  
423 ... Fereres, E. (2020, May). Irrigation of World Agricultural Lands: Evolution  
424 through the Millennia. *Water*, *12*(5), 1285. doi: 10.3390/w12051285
- 425 Arheimer, B., Donnelly, C., & Lindström, G. (2017, July). Regulation of snow-fed  
426 rivers affects flow regimes more than climate change. *Nature Communications*,  
427 *8*(1), 62. doi: 10.1038/s41467-017-00092-8
- 428 Beck, H. E., van Dijk, A. I. J. M., Levizzani, V., Schellekens, J., Miralles, D. G.,  
429 Martens, B., & de Roo, A. (2017, January). MSWEP: 3-hourly 0.25°&deg;  
430 global gridded precipitation (1979–2015) by merging gauge, satellite,  
431 and reanalysis data. *Hydrology and Earth System Sciences*, *21*(1), 589–615.  
432 doi: 10.5194/hess-21-589-2017
- 433 Beven, K. J., & Chappell, N. A. (2021). Perceptual perplexity and parameter parsimony.  
434 *WIREs Water*, *8*(4), e1530. doi: 10.1002/wat2.1530
- 435 Christidis, N., & Stott, P. A. (2022, August). Human Influence on Seasonal Precipitation  
436 in Europe. *Journal of Climate*, *35*(15), 5215–5231. doi: 10.1175/JCLI-D  
437 -21-0637.1
- 438 Collignan, J., Polcher, J., Bastin, S., & Quintana-Segui, P. (2023). Budyko Frame-  
439 work Based Analysis of the Effect of Climate Change on Watershed Evapora-  
440 tion Efficiency and Its Impact on Discharge Over Europe. *Water Resources*  
441 *Research*, *59*(10), e2023WR034509. doi: 10.1029/2023WR034509
- 442 Collignan, J., Polcher, J., Bastin, S., & Quintana-Seguí, P. (2023, August). *Out-*  
443 *put of the Land Surface Model ORCHIDEE over river catchments in Europe,*  
444 *run with GSWP3 and synthetic forcings where the precipitation is modified.*  
445 Zenodo. doi: 10.5281/zenodo.8211025
- 446 Coron, L., Andréassian, V., Perrin, C., Bourqui, M., & Hendrickx, F. (2014, Febru-  
447 ary). On the lack of robustness of hydrologic models regarding water balance  
448 simulation: A diagnostic approach applied to three models of increasing com-  
449 plexity on 20 mountainous catchments. *Hydrology and Earth System Sciences*,  
450 *18*(2), 727–746. doi: 10.5194/hess-18-727-2014
- 451 Dai, A. (2016). Historical and Future Changes in Streamflow and Continental  
452 Runoff. In *Terrestrial Water Cycle and Climate Change* (pp. 17–37). American  
453 Geophysical Union (AGU). doi: 10.1002/9781118971772.ch2
- 454 Dezi, Ş., Mindrescu, M., Petrea, D., Rai, P. K., Hamann, A., & Nistor, M.-M.  
455 (2018). High-resolution projections of evapotranspiration and water availabil-  
456 ity for Europe under climate change. *International Journal of Climatology*,  
457 *38*(10), 3832–3841. doi: 10.1002/joc.5537
- 458 Do, H. X., Zhao, F., Westra, S., Leonard, M., Gudmundsson, L., Boulange, J. E. S.,  
459 ... Wada, Y. (2020, April). Historical and future changes in global flood

- 460 magnitude – evidence from a model–observation investigation. *Hydrology and*  
 461 *Earth System Sciences*, 24(3), 1543–1564. doi: 10.5194/hess-24-1543-2020
- 462 Douville, H., Raghavan, K., Renwick, J., Allan, R., Arias, P., Barlow, M., . . . Zolina,  
 463 O. (2021). Water Cycle Changes. In *Climate Change 2021: The Physical*  
 464 *Science Basis. Contribution of Working Group I to the Sixth Assessment Re-*  
 465 *port of the Intergovernmental Panel on Climate Change.*, 1055–1210. doi:  
 466 10.1017/9781009157896.010
- 467 Esteban, E., & Albiac, J. (2012, August). The problem of sustainable groundwa-  
 468 ter management: The case of La Mancha aquifers, Spain. *Hydrogeology Jour-*  
 469 *nal*, 20(5), 851–863. doi: 10.1007/s10040-012-0853-3
- 470 Ficklin, D. L., Abatzoglou, J. T., Robeson, S. M., Null, S. E., & Knouft, J. H. (2018,  
 471 August). Natural and managed watersheds show similar responses to recent  
 472 climate change. *Proceedings of the National Academy of Sciences*, 115(34),  
 473 8553–8557. doi: 10.1073/pnas.1801026115
- 474 García-Ruiz, J. M., López-Moreno, J. I., Vicente-Serrano, S. M., Lasanta-Martínez,  
 475 T., & Beguería, S. (2011, April). Mediterranean water resources in a  
 476 global change scenario. *Earth-Science Reviews*, 105(3), 121–139. doi:  
 477 10.1016/j.earscirev.2011.01.006
- 478 Gudmundsson, L., Seneviratne, S. I., & Zhang, X. (2017, November). Anthropogenic  
 479 climate change detected in European renewable freshwater resources. *Nature*  
 480 *Climate Change*, 7(11), 813–816. doi: 10.1038/nclimate3416
- 481 Guimberteau, M., Laval, K., Perrier, A., & Polcher, J. (2012, September). Global  
 482 effect of irrigation and its impact on the onset of the Indian summer monsoon.  
 483 *Climate Dynamics*, 39(6), 1329–1348. doi: 10.1007/s00382-011-1252-5
- 484 Hagemann, S., & Dümenil, L. (1997, December). A parametrization of the lateral  
 485 waterflow for the global scale. *Climate Dynamics*, 14(1), 17–31. doi: 10.1007/  
 486 s003820050205
- 487 Han, J., Yang, Y., Roderick, M. L., McVicar, T. R., Yang, D., Zhang, S., & Beck,  
 488 H. E. (2020). Assessing the Steady-State Assumption in Water Balance  
 489 Calculation Across Global Catchments. *Water Resources Research*, 56(7),  
 490 e2020WR027392. doi: 10.1029/2020WR027392
- 491 Harris, I., Osborn, T. J., Jones, P., & Lister, D. (2020, April). Version 4 of the  
 492 CRU TS monthly high-resolution gridded multivariate climate dataset. *Scien-*  
 493 *tific Data*, 7(1), 109. doi: 10.1038/s41597-020-0453-3
- 494 Hegerl, G., & Zwiers, F. (2011). Use of models in detection and attribution of cli-  
 495 mate change. *WIREs Climate Change*, 2(4), 570–591. doi: 10.1002/wcc.121
- 496 Holtz, G., & Pahl-Wostl, C. (2012, March). An agent-based model of groundwa-  
 497 ter over-exploitation in the Upper Guadiana, Spain. *Regional Environmental*  
 498 *Change*, 12(1), 95–121. doi: 10.1007/s10113-011-0238-5
- 499 Huss, M., & Hock, R. (2018, February). Global-scale hydrological response to future  
 500 glacier mass loss. *Nature Climate Change*, 8(2), 135–140. doi: 10.1038/s41558  
 501 -017-0049-x
- 502 Hyungjun, K. (2017). Global Soil Wetness Project Phase 3 Atmospheric Boundary  
 503 Conditions (Experiment 1). *Data Integration and Analysis System (DIAS)*, 5.  
 504 doi: doi:10.20783/DIAS.501
- 505 Jiang, C., Xiong, L., Wang, D., Liu, P., Guo, S., & Xu, C.-Y. (2015, March). Sepa-  
 506 rating the impacts of climate change and human activities on runoff using the  
 507 Budyko-type equations with time-varying parameters. *Journal of Hydrology*,  
 508 522, 326–338. doi: 10.1016/j.jhydrol.2014.12.060
- 509 Krinner, G., Viovy, N., de Noblet-Ducoudré, N., Ogée, J., Polcher, J., Friedlingstein,  
 510 P., . . . Prentice, I. C. (2005). A dynamic global vegetation model for studies  
 511 of the coupled atmosphere-biosphere system. *Global Biogeochemical Cycles*,  
 512 19(1). doi: 10.1029/2003GB002199
- 513 Lawrence, D. M., Hurtt, G. C., Arneth, A., Brovkin, V., Calvin, K. V., Jones,  
 514 A. D., . . . Shevliakova, E. (2016, September). The Land Use Model Inter-

- 515 comparison Project (LUMIP) contribution to CMIP6: rationale and exper-  
 516 imental design. *Geoscientific Model Development*, 9(9), 2973–2998. doi:  
 517 10.5194/gmd-9-2973-2016
- 518 Lehner, B., Verdin, K., & Jarvis, A. (2008). New Global Hydrography Derived From  
 519 Spaceborne Elevation Data. *Eos, Transactions American Geophysical Union*,  
 520 89(10), 93–94. doi: 10.1029/2008EO100001
- 521 Llamas, M. R., Custodio, E., de la Hera, A., & Fornés, J. M. (2015, March).  
 522 Groundwater in Spain: Increasing role, evolution, present and future. *Envi-  
 523 ronmental Earth Sciences*, 73(6), 2567–2578. doi: 10.1007/s12665-014-4004-0
- 524 Luo, Y., Yang, Y., Yang, D., & Zhang, S. (2020, November). Quantifying the impact  
 525 of vegetation changes on global terrestrial runoff using the Budyko framework.  
 526 *Journal of Hydrology*, 590, 125389. doi: 10.1016/j.jhydrol.2020.125389
- 527 Milly, P. C. D., Dunne, K. A., & Vecchia, A. V. (2005, November). Global pat-  
 528 tern of trends in streamflow and water availability in a changing climate. *Na-  
 529 ture*, 438(7066), 347–350. doi: 10.1038/nature04312
- 530 Ministère de l’écologie, du développement durable et de l’énergie. (2021). *HYDRO*  
 531 [Dataset]. <https://www.hydro.eaufrance.fr/rechercher/entites-hydrometriques>.
- 532 Ministerio para la Transición Ecológica y el Reto Demográfico. (2020). *GeoPortal*.  
 533 <https://www.miteco.gob.es/es/cartografia-y-sig/ide/geoportal.html>.
- 534 Nazemi, A., & Wheeler, H. S. (2015, January). On inclusion of water resource  
 535 management in Earth system models &ndash; Part 1: Problem definition and  
 536 representation of water demand. *Hydrology and Earth System Sciences*, 19(1),  
 537 33–61. doi: 10.5194/hess-19-33-2015
- 538 Nguyen-Quang, T., Polcher, J., Ducharne, A., Arsouze, T., Zhou, X., Schneider, A.,  
 539 & Fita, L. (2018). ORCHIDEE-ROUTING: Revising the river routing scheme  
 540 using a high-resolution hydrological database. *Geoscientific Model Development  
 541 Discussions*, 11(12), 4965–4985. doi: 10.5194/gmd-11-4965-2018
- 542 Nicolle, P., Andréassian, V., Royer-Gaspard, P., Perrin, C., Thirel, G., Coron, L., &  
 543 Santos, L. (2021, September). Technical note: RAT – a robustness assessment  
 544 test for calibrated and uncalibrated hydrological models. *Hydrology and Earth  
 545 System Sciences*, 25(9), 5013–5027. doi: 10.5194/hess-25-5013-2021
- 546 Palmer, M. A., Reidy Liermann, C. A., Nilsson, C., Flörke, M., Alcamo, J., Lake,  
 547 P. S., & Bond, N. (2008). Climate change and the world’s river basins: Antic-  
 548 ipating management options. *Frontiers in Ecology and the Environment*, 6(2),  
 549 81–89. doi: 10.1890/060148
- 550 Perrin, C., Michel, C., & Andréassian, V. (2003, August). Improvement of a parsimonious  
 551 model for streamflow simulation. *Journal of Hydrology*, 279(1), 275–  
 552 289. doi: 10.1016/S0022-1694(03)00225-7
- 553 Polcher, J., Schrapffer, A., Dupont, E., Rinchiuso, L., Zhou, X., Boucher, O., ...  
 554 Servonnat, J. (2022, September). Hydrological modelling on atmospheric grids;  
 555 using graphs of sub-grid elements to transport energy and water. *EGUsphere*,  
 556 1–34. doi: 10.5194/egusphere-2022-690
- 557 Quintana-Seguí, P., Barella-Ortiz, A., Regueiro-Sanfiz, S., & Miguez-Macho, G.  
 558 (2020, May). The Utility of Land-Surface Model Simulations to Provide  
 559 Drought Information in a Water Management Context Using Global and Local  
 560 Forcing Datasets. *Water Resources Management*, 34(7), 2135–2156. doi:  
 561 10.1007/s11269-018-2160-9
- 562 Reaver, N. G. F., Kaplan, D. A., Klammler, H., & Jawitz, J. W. (2022, March).  
 563 Theoretical and empirical evidence against the Budyko catchment trajectory  
 564 conjecture. *Hydrology and Earth System Sciences*, 26(5), 1507–1525. doi:  
 565 10.5194/hess-26-1507-2022
- 566 Ribes, A., Thao, S., Vautard, R., Dubuisson, B., Somot, S., Colin, J., ... Soubey-  
 567 roux, J.-M. (2019, January). Observed increase in extreme daily rainfall  
 568 in the French Mediterranean. *Climate Dynamics*, 52(1), 1095–1114. doi:  
 569 10.1007/s00382-018-4179-2

- 570 Riedel, T., & Weber, T. K. D. (2020, September). Review: The influence of global  
571 change on Europe’s water cycle and groundwater recharge. *Hydrogeology Jour-*  
572 *nal*, 28(6), 1939–1959. doi: 10.1007/s10040-020-02165-3
- 573 Rottler, E., Francke, T., Bürger, G., & Bronstert, A. (2020, April). Long-  
574 term changes in central European river discharge for 1869–2016: Impact of  
575 changing snow covers, reservoir constructions and an intensified hydrolog-  
576 ical cycle. *Hydrology and Earth System Sciences*, 24(4), 1721–1740. doi:  
577 10.5194/hess-24-1721-2020
- 578 Rudolf, B., Beck, C., Grieser, J., Schneider, U., & Deutscher Wetterdienst, D.  
579 (2005). The Global Precipitation Climatology Centre (GPCC).
- 580 Schaner, N., Voisin, N., Nijssen, B., & Lettenmaier, D. P. (2012, September). The  
581 contribution of glacier melt to streamflow. *Environmental Research Letters*,  
582 7(3), 034029. doi: 10.1088/1748-9326/7/3/034029
- 583 Schneider, C., Laizé, C. L. R., Acreman, M. C., & Flörke, M. (2013, January). How  
584 will climate change modify river flow regimes in Europe? *Hydrology and Earth*  
585 *System Sciences*, 17(1), 325–339. doi: 10.5194/hess-17-325-2013
- 586 Siebert, S., Kummu, M., Porkka, M., Doell, P., Ramankutty, N., & Scanlon,  
587 B. (2015, March). A global data set of the extent of irrigated land from  
588 1900 to 2005. *Hydrology and Earth System Sciences*, 19, 1521–1545. doi:  
589 10.5194/hess-19-1521-2015
- 590 Stephens, G., Polcher, J., Zeng, X., van Oevelen, P., Poveda, G., Bosilovich, M.,  
591 ... Bony, S. (2023, January). The First 30 Years of GEWEX. *Bul-*  
592 *letin of the American Meteorological Society*, 104(1), E126-E157. doi:  
593 10.1175/BAMS-D-22-0061.1
- 594 Tafasca, S., Ducharne, A., & Valentin, C. (2020, July). Weak sensitivity of the  
595 terrestrial water budget to global soil texture maps in the ORCHIDEE land  
596 surface model. *Hydrology and Earth System Sciences*, 24(7), 3753–3774. doi:  
597 10.5194/hess-24-3753-2020
- 598 Vicente-Serrano, S. M., Peña-Gallardo, M., Hannaford, J., Murphy, C., Lorenzo-  
599 Lacruz, J., Dominguez-Castro, F., ... Vidal, J.-P. (2019). Climate, Irrigation,  
600 and Land Cover Change Explain Streamflow Trends in Countries Bordering  
601 the Northeast Atlantic. *Geophysical Research Letters*, 46(19), 10821–10833.  
602 doi: 10.1029/2019GL084084
- 603 Vincent, C., Fischer, A., Mayer, C., Bauder, A., Galos, S. P., Funk, M., ... Huss,  
604 M. (2017). Common climatic signal from glaciers in the European Alps  
605 over the last 50 years. *Geophysical Research Letters*, 44(3), 1376–1383. doi:  
606 10.1002/2016GL072094
- 607 Wang, F., Polcher, J., Peylin, P., & Bastrikov, V. (2018, July). Assimilation of  
608 river discharge in a land surface model to improve estimates of the continental  
609 water cycles. *Hydrology and Earth System Sciences*, 22(7), 3863–3882. doi:  
610 10.5194/hess-22-3863-2018
- 611 Wang, W., Zhang, Y., & Tang, Q. (2020, December). Impact assessment of climate  
612 change and human activities on streamflow signatures in the Yellow River  
613 Basin using the Budyko hypothesis and derived differential equation. *Journal*  
614 *of Hydrology*, 591, 125460. doi: 10.1016/j.jhydrol.2020.125460
- 615 Weedon, G. P., Balsamo, G., Bellouin, N., Gomes, S., Best, M. J., & Viterbo, P.  
616 (2014). The WFDEI meteorological forcing data set: WATCH Forcing Data  
617 methodology applied to ERA-Interim reanalysis data. *Water Resources Re-*  
618 *search*, 50(9), 7505–7514. doi: 10.1002/2014WR015638
- 619 Xiong, M., Huang, C.-S., & Yang, T. (2020, June). Assessing the Impacts of Climate  
620 Change and Land Use/Cover Change on Runoff Based on Improved Budyko  
621 Framework Models Considering Arbitrary Partition of the Impacts. *Water*,  
622 12(6), 1612. doi: 10.3390/w12061612
- 623 Zanardo, S., Harman, C. J., Troch, P. A., Rao, P. S. C., & Sivapalan, M. (2012).  
624 Intra-annual rainfall variability control on interannual variability of catchment

- 625 water balance: A stochastic analysis. *Water Resources Research*, 48(6). doi:  
626 10.1029/2010WR009869
- 627 Zhang, L., Hickel, K., Dawes, W. R., Chiew, F. H. S., Western, A. W., & Briggs,  
628 P. R. (2004). A rational function approach for estimating mean annual  
629 evapotranspiration. *Water Resources Research*, 40(2). doi: 10.1029/  
630 2003WR002710
- 631 Zhang, L., Potter, N., Hickel, K., Zhang, Y., & Shao, Q. (2008, October). Water  
632 balance modeling over variable time scales based on the Budyko framework –  
633 Model development and testing. *Journal of Hydrology*, 360(1), 117–131. doi:  
634 10.1016/j.jhydrol.2008.07.021
- 635 Zhao, J., Huang, S., Huang, Q., Wang, H., & Leng, G. (2018, September). De-  
636 tecting the Dominant Cause of Streamflow Decline in the Loess Plateau  
637 of China Based on the Latest Budyko Equation. *Water*, 10(9), 1277. doi:  
638 10.3390/w10091277
- 639 Zhao, W., & Li, A. (2015, August). A Review on Land Surface Processes Modelling  
640 over Complex Terrain. *Advances in Meteorology*, 2015, e607181. doi: 10.1155/  
641 2015/607181
- 642 Zheng, Y., Huang, Y., Zhou, S., Wang, K., & Wang, G. (2018, December). Ef-  
643 fect partition of climate and catchment changes on runoff variation at the  
644 headwater region of the Yellow River based on the Budyko complemen-  
645 tary relationship. *Science of The Total Environment*, 643, 1166–1177. doi:  
646 10.1016/j.scitotenv.2018.06.195
- 647 Zveryaev, I. I. (2004). Seasonality in precipitation variability over Europe. *Journal*  
648 *of Geophysical Research: Atmospheres*, 109(D5). doi: 10.1029/2003JD003668

# Supporting Information for ”Identifying and quantifying the impact of climatic and non-climatic drivers on river discharge in Europe”

Julie Collignan<sup>1</sup>, Jan Polcher<sup>1</sup>, Sophie Bastin<sup>2</sup>, Pere Quintana-Segui<sup>3</sup>

<sup>1</sup>Laboratoire de Météorologie Dynamique/IPSL - Ecole Polytechnique/CNRS -, Paris, France

<sup>2</sup>Laboratoire Atmosphères, Observations Spatiales/IPSL - CNRS -, Paris, France

<sup>3</sup>Observatori de l'Ebre (Universitat Ramon Llull – CSIC), Roquetes, Spain

## Contents of this file

1. Complements on validation and robustness of the method
2. Map of the specific catchments referred to in the study
3. Illustration of the analysis at the catchment level

## Introduction

This supplementary information file contains a complementary explanation of the sensitivity and robustness tests done for the study. It also includes a map of the catchments specifically referred to in the article. Finally, it includes a detailed illustration of the methodology at the catchment scale for a given catchment in Northern Spain.

---

## Complements on validation and robustness of the method

### a- Adequacy of the framework

The method aims to compare the trends in river discharge  $Q_{LSM}$  from the model, which represents the climatic conditions only, and  $Q_{obs}$  deduced from observations, which represent all conditions at once, the actual conditions. They are not compared directly but through their substitutes  $Q_{climat}$  and  $Q_{actual}$  determined with the Budyko framework, which facilitates the interpretation of partial trends. We, therefore, need to attest to the quality of the Budyko framework to reproduce  $Q_{LSM}$  and  $Q_{obs}$  through their parametric representation.

We use the Nash-Sutcliffe coefficient (NSC) and the Percent bias (PBIAS) (Fig. S1). The Budyko framework is able to reproduce correctly the annual mean of observed river discharge over all European basins with a very good PBIAS ( $<10\%$  for all river basins) (Fig. S1d) and a good NSC  $> 0.5$  for 569 stations out of 849, except for north-eastern Europe, where we locate the majority of stations which fail this test (Fig. S1c). This second test is more demanding and attests to the quality of Budyko framework to reproduce the inter-annual variations of discharge. It is also efficient to reproduce the climatic river discharge from the model (Fig. S1a and S1b) with  $NSC > 0.5$  and  $PBIAS \leq 15\%$  except for a few basins and still an under-performance for NSC over Eastern Europe.

Therefore, the Budyko framework is an adequate parametric representation of annual mean discharge in both systems and we can use  $Q_{climat}$  and  $Q_{actual}$  derived from this framework to compare the climatic behavior of the watershed and its actual behavior.

In this study, we filter out the stations for which  $NSC < 0.5$ . We only keep the 569 stations for which the Budyko framework is efficient for both reproducing  $Q_{LSM}$  and  $Q_{obs}$ . Therefore, the analysis when comparing  $Q_{climat}$  and  $Q_{total}$  will not be tinted by the ability of Budyko framework to effectively reproduce  $Q_{LSM}$  and  $Q_{obs}$  respectively.

### **b- Robustness to climate data**

We also tested the method's robustness and its sensitivity to data driving the LSM by comparing its application with different forcing datasets. Three independent atmospheric datasets are available over the 1979-2010 period.

Over such a short period, trends are mostly non-significant and can't be appropriately statistically compared. However, for all forcings considered, the patterns are very similar. Here we focus on the efficiency parameters  $\omega_c$  and  $\omega_a$  correlation and variance for each forcing, to analyze the impact of the forcing choice on how our method attributes variations of  $\omega$  to climatic behavior with our LSM.

Comparing  $\omega_c$  and  $\omega_a$  obtained for the three forcings over the common period and for each system, we obtain very similar results when looking at the average variance over all basins for each evapotranspiration efficiencies time-series and the two-by-two correlations (Tab. S1).

The variances have a similar order of magnitude no matter the forcing used to calculate  $\omega_c$  and  $\omega_a$ , consistently producing  $\omega_a$  larger than  $\omega_c$  by a factor of ten with all forcings. E2OFD has a finer resolution, increasing the results' variability relative to the other two coarser climate datasets. The forcing datasets are not fully independent given the limited

number of observations. For instance, GSWP3 and WFDEI use the same precipitation product to bias correct the re-analyses on which they are based. E2OFD and WFDEI use the same re-analysis but interpolated to different resolutions and corrected with two distinct observational precipitation estimates. Given that the results are closer for GSWP3 and WFDEI, we can hypothesize that the method is more sensitive to the precipitation data used than the other variables.

These results show globally that the method is robust, since it is not very sensitive to the forcing used. The differences in variance between forcings are smaller than those between the variance of  $\omega_a$  and  $\omega_c$  for all tested forcings. The poorest correlation is between E2OFD and GSWP3 (the forcings most different from each other) and mostly for  $\omega_c$ , which has the smallest average variance. Therefore, it will impact our results less when comparing trends. However, the absolute values of  $\omega$  are significantly different depending on the forcing used, comforting the idea that this method can only be used to assess and compare trends.

Results presented in the article are obtained with the forcing dataset GSWP3, which covers the longest time period 1901-2012 and is thus most relevant for evaluating the driver of river discharge trends.

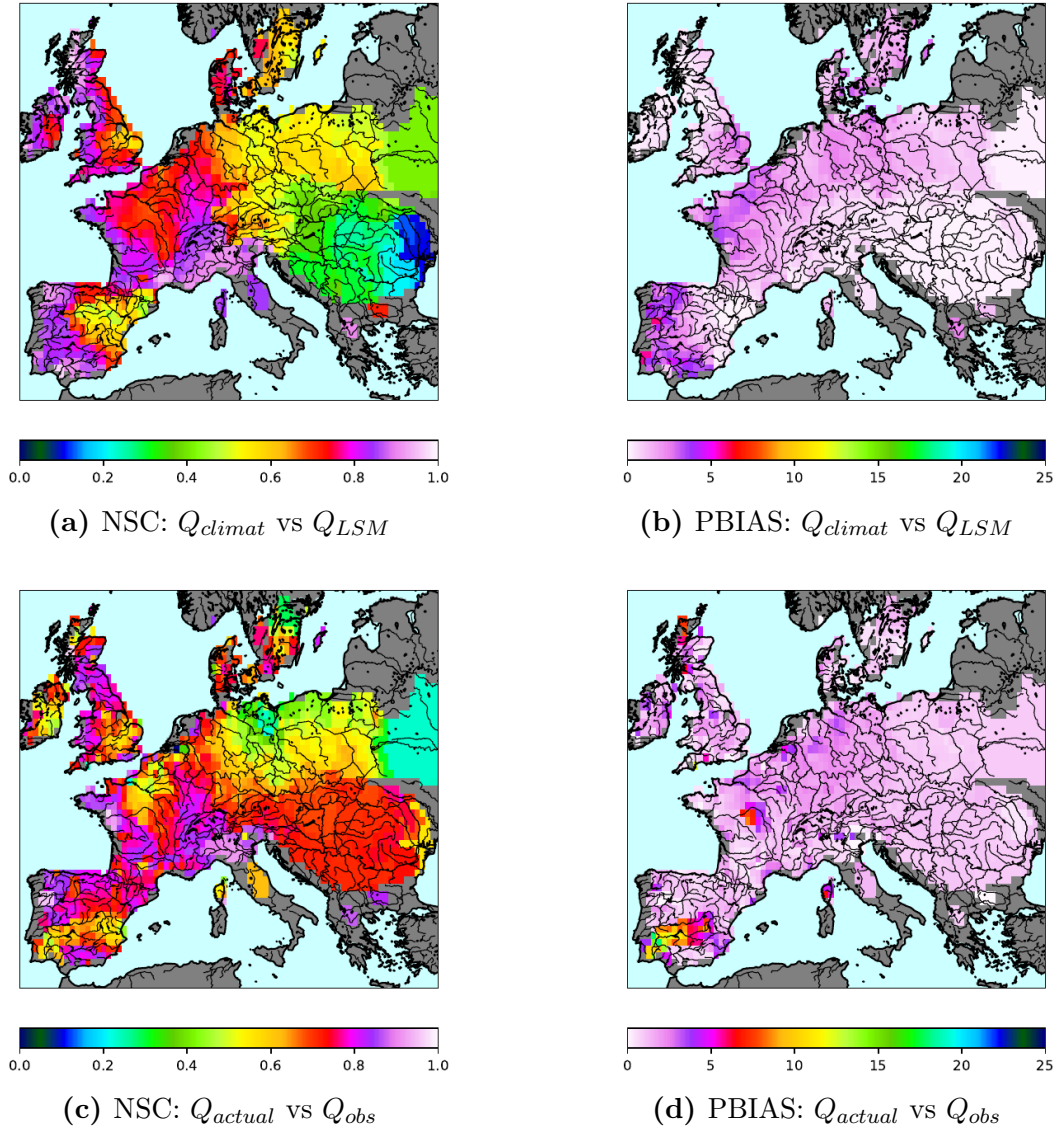


**Figure S1.** Using Nash-Sutcliffe coefficient (NSC) and absolute Percent bias (PBIAS) to compare river discharge modelled  $Q_{LSM}$  or observed  $Q_{obs}$  to river discharge  $Q_{climat}$  and  $Q_{actual}$  calculated with Fu's equation, to attest the quality of the Budyko framework. Colors from yellow to pink are considered as satisfactory.

February 1, 2024, 2:43pm

**Table S1.** Comparison of the evaporation efficiencies time-series calculated with the different forcings for each system over the period 1979-2010:  $\omega_c$  for the climatic system and  $\omega_a$  for the actual system.

Average variance over all catchments

	$\omega_c$	$\omega_a$
GSWP3	0.0023	0.039
WFDEI	0.0033	0.036
E2OFD	0.0110	0.031

Correlations:

% of stations with average correlation  $> 0.6$  and median correlation between all catchments

		$\omega_c$		$\omega_a$
E2OFD/GSWP3	38%	0.50	53%	0.65
WFDEI/GSWP3	73%	0.75	77%	0.99
E2OFD/WFDEI	64%	0.70	59%	0.73

## Map of the specific catchments referred to in the study

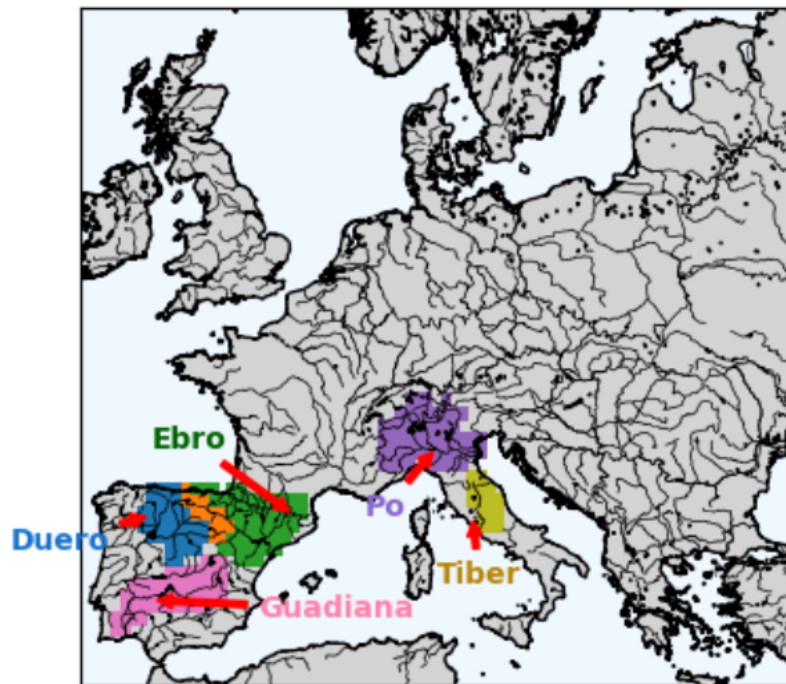


**Figure S2.** Catchments of specific rivers in Spain (Ebro, Duero, Guadiana) and Italy (Tiber, Po), referred to in the article as specific examples of some results and hypotheses.

### Illustration of the analysis at the catchment level

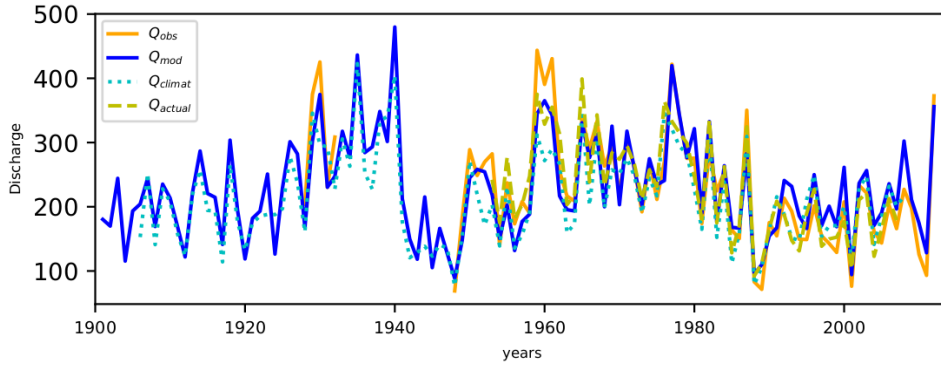
The discharge (Fig. S3b) at the station level has continuous observations from the 1950's ( $Q_{obs}$ ). We see that if the variability of  $Q_{obs}$  and  $Q_{mod}$  are very similar (Fig. S3b), we see that over the observation period covered by the observation, at the beginning of the period (1950-1970),  $Q_{obs} > Q_{mod}$  while at the end of the period (1990-2010),  $Q_{obs} < Q_{mod}$ . Both tend to decrease but  $Q_{obs}$  has a steeper decrease. Looking at the variations of  $\omega$  (Fig. S3c) in both systems helps to explain that difference.  $\omega_c$  is not constant over time but its variability is smaller than that of  $\omega_a$ . There are other non-climatic factors inducing higher trends. For the particular case of Castejon, there are two time periods at the end of the 1960's end in the 1985-1995 period

where there are trends in  $\omega_a$  with a slope which is higher than 90% of all of  $\omega_c$  slopes over the entire century (Fig. S3d). Therefore, there is a high probability that these slopes can not be explained only by climatic phenomena. They are positive trends: non-climatic factors tend to increase evaporation efficiency (associated with a decrease in discharge, not significant, however, at the decadal scale).

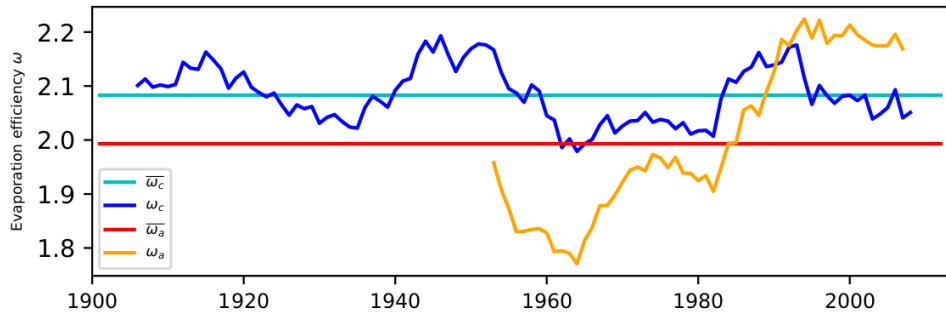
6226300: Ebro, Rio : Castejon, Lon: -1.69° Lat: 42.18° ES



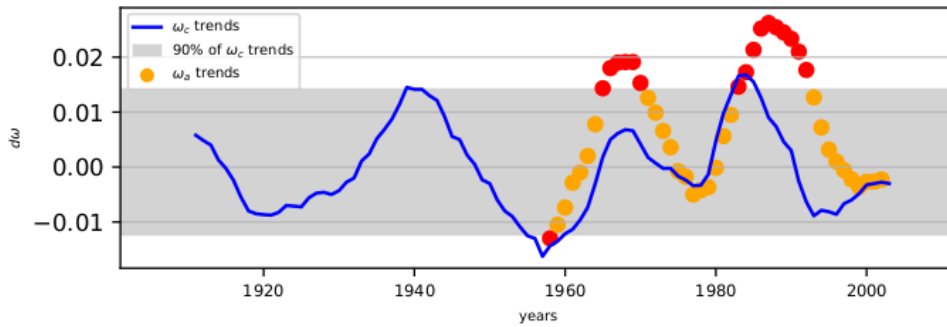
(a) Watershed of the gauging station Castejon on the Ebro river



(b) Discharge at the station outlet: Observed discharge  $Q_{obs}$  (orange), modeled discharge from the LSM ORCHIDEE  $Q_{mod}$  (blue) and from the Budyko framework fitted on the model  $Q_{climat}$  (dotted blue) and on the observations  $Q_{actual}$  (dashed orange)



(c)  $\omega$  fitted on the model outputs ( $\omega_c$  (blue) corresponding to the "climatic"  $\omega$ , compared to  $\omega_a$  (orange) fitted on the observations).



(d) Slopes of  $\omega$  calculated with an 11-year time moving window (slope calculated over 11 years, 5 years prior and after the referenced year), for  $\omega_c$  (blue) and for  $\omega_a$  (orange). The red points corresponds to years for which the absolute slope of  $\omega_a$  is different from 90% of all  $\omega_c$  slopes (grey area).

February 1, 2024, 2:43pm

**Figure S3.** Example of the results at the station level for the gauging station Castejon on the Ebro river in Spain